



University of  
Massachusetts  
Amherst

## Quark and lepton masses and mixing in the landscape

Item Type	article
Authors	Donoghue, JF;Dutta, K;Ross, A
Download date	2026-04-21 23:21:01
Link to Item	<a href="https://hdl.handle.net/20.500.14394/41115">https://hdl.handle.net/20.500.14394/41115</a>

# Quark and lepton masses and mixing in the landscape

John F. Donoghue, Koushik Dutta and Andreas Ross

Department of Physics  
University of Massachusetts  
Amherst, MA 01003, USA

February 2, 2008

## Abstract

Even if quark and lepton masses are not uniquely predicted by the fundamental theory, as may be the case in the string theory landscape, nevertheless their pattern may reveal features of the underlying theory. We use statistical techniques to show that the observed masses appear to be representative of a scale invariant distribution,  $\rho(m) \sim 1/m$ . If we extend this distribution to include all the Yukawa couplings, we show that the resulting CKM matrix elements typically show a hierarchical pattern similar to observations. The Jarlskog invariant measuring the amount of CP violation is also well reproduced in magnitude. We also apply this framework to neutrinos using the seesaw mechanism. The neutrino results are ambiguous, with the observed pattern being statistically allowed even though the framework does not provide a natural explanation for the observed two large mixing angles. Our framework highly favors a normal hierarchy of neutrino masses. We also are able to make statistical predictions in the neutrino sector when we specialize to situations consistent with the known mass differences and two large mixing angles. Within our framework, we show that with 95% confidence the presently unmeasured MNS mixing angle  $\sin\theta_{13}$  is larger than 0.04 and typically of order 0.1. The leptonic Jarlskog invariant is found to be typically of order  $10^{-2}$  and the magnitude of the effective Majorana mass  $m_{ee}$  is typically of order 0.001 eV.

# 1 Introduction

Of the 28 parameters of the Standard Model (including neutrino masses and mixing) the quark and lepton masses appear particularly puzzling. We would expect that the spectrum of masses would exhibit some underlying structure, much as the periodic table and the hadron spectrum respectively reveal the dynamics of atoms and elementary particles. However, apparently the quark and lepton masses do not show any such pattern. Aside from a rough correlation of mass with generation, decades of searching have not revealed any significant regularity in the masses. Perhaps there is none.

In this paper, we explore the possibility that the masses and mixings are not uniquely predicted, but are representative of an ensemble of possibilities. The masses and mixing then reveal the “weight” or “measure” of the underlying theory. This possibility was first proposed by Donoghue in [1], and we develop it further. This is a plausible outcome of the string theory landscape [2]. In this description, there are very many Standard Model vacua with parameters close to those observed, and yet many more with different parameters. While we observe only a single ground state, the solution that we observe is representative of the ensemble of possible SM vacua that occur in the landscape. In particular, the Yukawa couplings would not be unique, but would be representative of the couplings found in the ensemble of solutions. Since we have many manifestations of the Yukawa couplings (9 quark and lepton masses, two neutrino mass differences as well as the CKM and MNS weak mixing elements) we may apply statistical methods even though we live in a single member of the possible landscape vacua. Our primary assumption is that the observed masses are representative of this ensemble. By studying the phenomenology of the masses, we then learn about the nature of the underlying theory.

By employing statistical tests we will show that the observed quark masses appear to be distributed in a scale-invariant fashion. This was already suggested in [1] but we provide better statistical measures. This result can be readily seen in Fig. 1. A scale invariant set of masses is one where the values appear as a uniform random distribution when plotted on a log scale. The masses of the quarks and charged leptons are shown on such a scale in Fig. 1 and appear visually to be consistent with being uniformly random. In Section 3, we use statistical tests to confirm this and to quantify how far the weight could deviate from a scale invariant form. In Section 4 we apply this distribution to the full Yukawa matrices of quarks and investigate the weak mixing angles. We will see that one naturally generates a hierarchy in the CKM elements similar to the one found in nature, aside from a discrete ambiguity concerning the generation structure. Moreover, the magnitude of the observed CP violation is readily reproduced.

The neutrino masses appear quite different from other lepton masses, with a possible explanation being the seesaw mechanism and the presence of heavy right handed Majorana mass. We explore the neutrino masses in a similar fashion, using the same weight for the Dirac masses and allowing a different weight for the Majorana masses. We describe the neutrino phenomenology in Section 5.

It is possible that these results could be useful in testing or exploring the string landscape. For example, it has been suggested [3] that a scale invariant weight could emerge from the intersecting brane worlds construction [4] of the Standard Model. If some branches of the landscape yield weights compatible with observations while others do not, this could be used to refine our location in the space of string theory solutions. We are clearly far from an understanding of the landscape, but the masses and mixings of the leptons can play a useful role in landscape phenomenology.

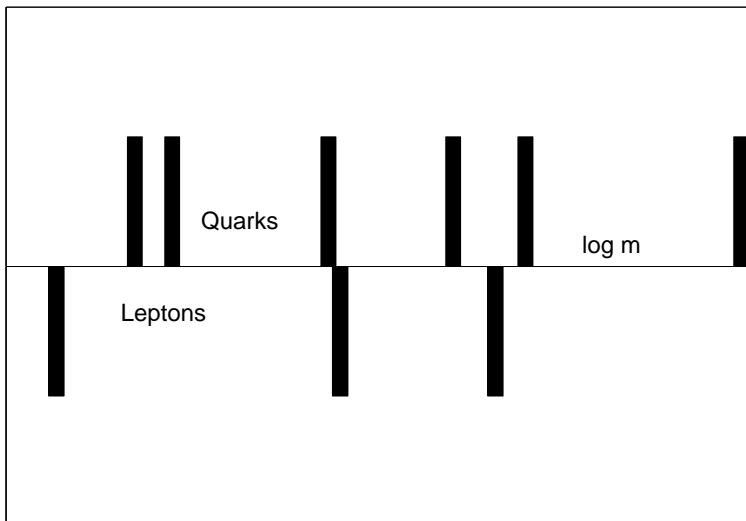


Figure 1: Quark and lepton masses, defined at the energy  $\mu = M_W$ , on a logarithmic scale. A scale invariant weight corresponds to a uniform distribution on this scale.

## 2 The properties of the weight

The most fundamental assumption of our approach is the existence of a large ensemble of nearly equivalent vacuum states with different values of the quark masses, of which our vacua is assumed to be representative. The string landscape could be such a theory. It has been estimated [2] that there are perhaps  $10^{100}$  Standard Model vacua with parameters agreeing with observation within the experimental error bars. There are then many more that look like the Standard Model but have other values of the quark and lepton masses. This larger set of SM vacua then constitutes our ensemble.

Within this ensemble we need to make other assumptions. For example, we are assuming that the quark masses are not correlated with each other. If there are really of order  $10^{100}$  vacua this seems reasonable. We could hold any one of the quark masses fixed and still find a whole range of values for the other masses. We also will make the assumption that quark and charged lepton masses (but not neutrino masses) play by the same rules, although we will explore some slight differences that arise due to the differences between quarks and leptons. Finally, we need to make assumptions about the whole matrix of Yukawa couplings, as will be discussed below.

The weight  $\rho(m)$  is a probability distribution function for the masses (or later for the Yukawa couplings). It is defined by considering the fraction of masses  $f$  found at a value  $m$  within  $dm$  as

$$f(m) = \rho(m)dm. \quad (1)$$

The normalization of the weight is by definition then

$$1 = \int \rho(m)dm. \quad (2)$$

For the simple weights  $\rho(m)$  that we consider, this normalization condition demands upper limits and, in some cases, lower limits for the range of allowed masses.

Because the masses depend on the energy scale, the weight will also depend on this scale. The renormalization group allows us to determine the scale dependence, as was shown

in [1]. When the energy scale is changed from  $\mu_1$  to  $\mu_2$  a mass  $m_1$  will change to the value  $m_2$ , defining a functional relationship  $m_2 = m_2(m_1)$  or the reverse  $m_1 = m_1(m_2)$ . In order to preserve the definition of the weight, it must transform as

$$\rho_{\mu_2}(m_2) = \rho_{\mu_1}(m_1(m_2))J(m_2) \quad (3)$$

with

$$J = \frac{\partial m_1}{\partial m_2}. \quad (4)$$

As an example, under QCD the masses transform as

$$m(\mu_2) = m(\mu_1) \left[ \frac{\alpha_s(\mu_2)}{\alpha_s(\mu_1)} \right]^{d_m} \quad (5)$$

with

$$d_m = \frac{4}{11 - \frac{2N_f}{3}}. \quad (6)$$

In this case the renormalization group transformation rule yields

$$\rho_{\mu_2}(m) = \rho_{\mu_1} \left( m \left[ \frac{\alpha_s(\mu_2)}{\alpha_s(\mu_1)} \right]^{-d_m} \right) \left[ \frac{\alpha_s(\mu_2)}{\alpha_s(\mu_1)} \right]^{-d_m}. \quad (7)$$

For large values of the masses we also need to consider the effect of the Yukawa interaction on its own running. Recall that in the Standard Model the masses  $m_i$  are related to the Yukawa couplings  $h_i$  via  $m_i = h_i \frac{v}{\sqrt{2}}$  where  $v$  is the Higgs vev. The renormalization group equations for the combined QCD gauge and Yukawa running for  $N_f = 6$  are

$$\begin{aligned} \frac{dg_3^2}{dt} &= \frac{7}{16\pi^2} g_3^4 \\ \frac{dh^2}{dt} &= h^2 \left( \frac{1}{2\pi^2} g_3^2 - \frac{9}{32\pi^2} h^2 \right) \end{aligned} \quad (8)$$

where  $t = \log(\mu_1^2/\mu^2)$ , using  $\mu_1$  as the initial scale. Note that the QCD interaction tends to make the Yukawa coupling larger as one scales down in energy ( $t$  positive), while the Yukawa self interaction tends to make the Yukawa coupling smaller. One of the consequences of this is the well known quasi-fixed-point [5] at  $m_* = 220$  GeV - all large Yukawa couplings will run to a value close to this fixed point when scaled down from large energy to the  $W$  scale. The solution to the Yukawa RGE has the form [5]

$$\begin{aligned} h(t) &= \frac{b(t)h(0)}{[1 + a(t)h^2(0)]^{1/2}} \\ b(t) &= \left( \frac{\alpha_s(t)}{\alpha_s(0)} \right)^{4/7} \\ a(t) &= \frac{9}{2g_3^2(0)} \left[ \left( \frac{\alpha_s(t)}{\alpha_s(0)} \right)^{1/7} - 1 \right]. \end{aligned} \quad (9)$$

From this we can extract the Jacobian for the weight

$$J(m) = \frac{b^2}{\left[ b^2 - 2a \frac{m^2}{v^2} \right]^{3/2}}. \quad (10)$$

For small masses, this is equivalent to the gauge rescaling given above. For leptons, we neglect the QED effects and only consider the Yukawa interaction. In this case, the above formulas continue to hold, but with the identification

$$\begin{aligned} b(t) &= 1 \\ a(t) &= \frac{9}{32\pi^2} t. \end{aligned} \quad (11)$$

Let us look at a particular weight which plays an important role in the rest of this paper. This is a weight that has the form  $\rho(m) \sim 1/m$ , which we will call the *scale invariant* weight. To normalize this form we need to limit the range of masses with an upper and a lower cutoff, so that the complete form is

$$\rho(m) = \frac{1}{\log \frac{m_+}{m_-}} \frac{1}{m} \Theta(m - m_-) \Theta(m_+ - m). \quad (12)$$

This distribution is scale invariant in two senses. First, a probability distribution that goes as  $dm/m$  is clearly invariant under a rescaling of all masses  $m \rightarrow \lambda m$ . The endpoints are not invariant but they rescale in the obvious fashion. In addition, this weight is invariant under renormalization group transformation of the gauge interactions changing from one scale  $\mu_1$  to another scale  $\mu$ . This can be seen simply from Eq. (7).

However, the Yukawa interactions modify the shape of this weight. In particular, if the weight takes the above form at a scale  $\mu_1$ , then at a lower scale  $\mu$  it will have the form

$$\rho_\mu(m) = \left[ \frac{1}{1 - 2a \frac{m^2}{b^2 v^2}} \right] \frac{1}{\log \frac{m_+}{m_-}} \frac{1}{m} \Theta(m - \hat{m}_-) \Theta(\hat{m}_+ - m) \quad (13)$$

where

$$\hat{m}_\pm = \frac{bm_\pm}{\left[1 + 2a \frac{m_\pm^2}{v^2}\right]^{1/2}} \quad (14)$$

are the rescaled endpoints.

We can illustrate the renormalization group effects by considering the transformation from a Grand Unified scale of  $\mu = 10^{16}$  GeV down to the  $W$  scale. At the GUT scale we postulate for the Yukawa couplings the weight

$$\rho_\mu(h) = \frac{1}{\log \frac{h_+}{h_-}} \frac{1}{h} \Theta(h - h_-) \Theta(h_+ - h) \quad (15)$$

with  $h_+ = 1$  and  $h_- = 1.2 \times 10^{-6}$ . The values of the endpoints have been chosen to allow the mass ranges to extend from below the electron mass to above the top quark mass. When transformed down to the  $W$  scale, the maximum value of the quark mass distribution is  $\hat{m}_+ = 197$  GeV and the minimum value is  $\hat{m}_- = 0.53$  MeV. For the leptons, the corresponding values are  $\hat{m}_+ = 103$  GeV and  $\hat{m}_- = 0.20$  MeV. Note that the rescaled ranges of the distributions are different for quarks and leptons. At low values of the mass the weight retains the  $1/m$  form, but the larger values the shape of the distribution is modified. This is shown in Fig. 2 (a) for the quarks and Fig. 2 (b) for the leptons. The modification to the shape is gentle enough that we will ignore it in most of the phenomenological applications below. However, in the next section we will briefly explore the effect of rescaling the quark and lepton masses to the GUT scale and fitting the weight at that scale.

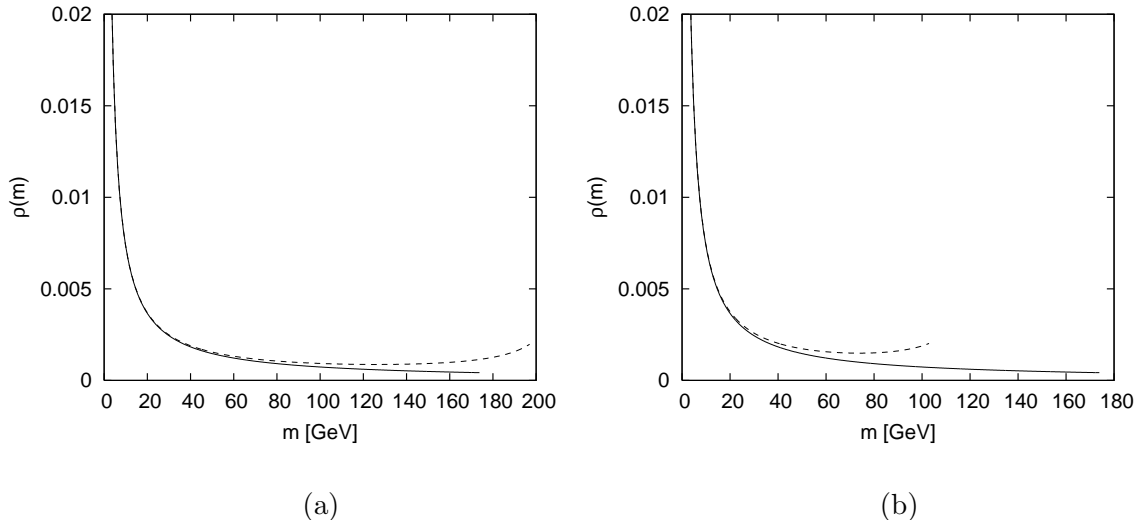


Figure 2: (a) The solid curve corresponds to a pure scale invariant weight with an maximum Yukawa coupling of 1 and a minimum of  $1.2 \times 10^{-6}$ . The dashed curve corresponds to using such a weight defined at the GUT scale and evolving it down to the  $W$  scale using the renormalization group equations for quarks. Note the slight distortion of the shape as well as the shift in the endpoints of the distribution. (b) Same as before, except that the renormalization group for leptons was applied.

### 3 Quark and charged lepton masses

In this section we will treat the quark and charged lepton masses and will determine the weight that best describes their distribution. We describe the masses at the scale of  $M_W$ . Running the quark masses to  $M_W$  the dominant contributions come from QCD running and we can neglect electroweak running for our purposes. The quark masses at the scale  $M_W$  [1] are given in Table 1. For leptons we neglect the small effects on the masses from electroweak running so that the lepton masses we use at  $M_W$  are simply the ones quoted by the PDG [10] as given in Table 2.

$m_u$	$m_d$	$m_s$	$m_c$	$m_b$	$m_t$
2.2 MeV	4.4 MeV	80 MeV	0.81 GeV	3.1 GeV	170 GeV

Table 1: Quark masses at the scale  $M_W$ .

$m_e$	$m_\mu$	$m_\tau$
0.511 MeV	0.106 GeV	1.78 GeV

Table 2: Lepton masses at the scale  $M_W$ .

From these values, we can deduce several properties. The masses span a range of more than five orders of magnitude, from  $m_e$  to  $m_t$ . Most obviously, the weight is not flat, but it must be peaked towards low masses. It is also not likely to be a Gaussian or an exponential, because such distributions would have an exponentially small probability of accommodating

the top quark. The weight must have a peak at low mass, yet extend out to high mass in order to explain the top quark.

We will explore the class of power law weights, and will see that they are successful in describing the distribution in masses. The power law weights have the form

$$\rho(m) \sim \frac{1}{m^\delta}. \quad (16)$$

Obviously they are not normalizable if the range includes all values of  $m$ , so we need to limit the range of the values of masses  $m$ . For  $\delta \leq 1$  we need an upper bound of the range of  $m$  so that the weight is normalizable. A natural choice for that is the quasi fixed point of the SM,  $m_* = 220$  GeV, which we will use as an upper bound for masses for all values of  $\delta$ . For  $\delta \geq 1$  we also need a lower bound for the range of  $m$ . In order to explain the existence of the electron but no lighter fermions, a sensible value for the lower bound should be smaller than  $m_e$  but not by many orders of magnitude. We choose  $m_{low} = 0.4 \cdot m_e$  [1] where  $m_e$  is the electron mass. Varying this value does not significantly affect the conclusions presented in this section. Using these bounds and normalizing the weight, we obtain the correct expressions for power law weights:

A) for  $\delta = 1$ :

$$\rho(m) = \frac{1}{\log \frac{m_*}{m_{low}}} \frac{1}{m} \Theta(m - m_{low}) \Theta(m_* - m) \quad (17)$$

B) for  $\delta \neq 1$  with a lower bound  $m_{low}$ :

$$\rho(m) = \frac{1 - \delta}{m_*^{1-\delta} - m_{low}^{1-\delta}} \frac{1}{m^\delta} \Theta(m - m_{low}) \Theta(m_* - m) \quad (18)$$

C) for  $\delta < 1$  without a lower bound  $m_{low}$ :

$$\rho(m) = \frac{1 - \delta}{m_*^{1-\delta}} \frac{1}{m^\delta} \Theta(m_* - m) \quad (19)$$

The distribution of a sample of random numbers with a power law weight  $\rho(m) \sim \frac{1}{m^\delta}$  looks like a uniformly distributed sample on the scale  $m^{1-\delta}$  (for  $\delta \neq 1$ ). For the scale invariant weight  $\rho(m) \sim \frac{1}{m}$ , a sample looks uniformly distributed on the scale  $\log m$ . Fig. 1 shows the physical masses of the quarks and leptons on a log scale and it is visible that these are consistent with a uniform distribution. For contrast, in Fig. 3 we plot the quark and lepton masses on a  $\sqrt{m}$  scale which corresponds to a weight  $\rho(m) \sim \frac{1}{\sqrt{m}}$ . It is evident that this sample is quite unlikely to result from a uniform random distribution.

We can make this mathematically precise by using the maximum likelihood method to select the optimum power  $\delta$ . The likelihood function is defined as the product of the weights of the masses:

$$L(\delta) = \prod_{i=u,d,s,c,b,t} \rho(m_i, \delta) \quad \text{for quarks only} \quad (20)$$

$$L(\delta) = \prod_{i=e,\mu,\tau,u,d,s,c,b,t} \rho(m_i, \delta) \quad \text{for quarks and leptons} \quad (21)$$

The optimum power delta is where  $L(\delta)$  has a maximum  $L_{max}$ , which coincides with the maximum of the log likelihood function  $\log L(\delta)$ . The one sigma range is limited by the

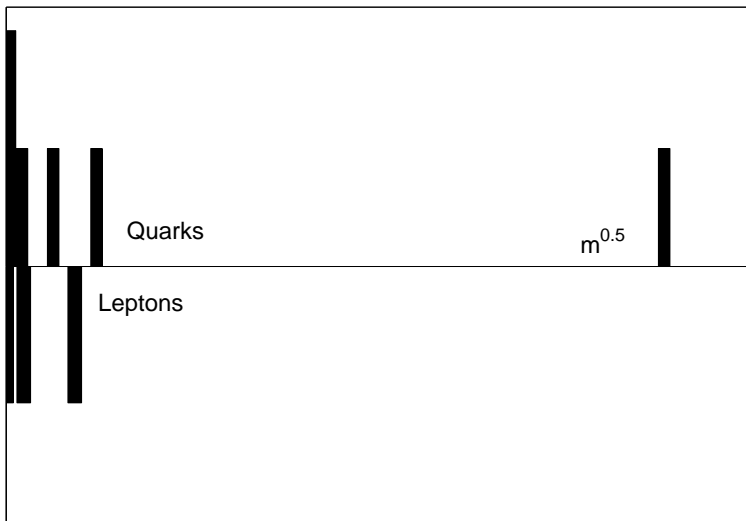


Figure 3: Quark and lepton masses, defined at the energy  $\mu = M_W$ , plotted versus  $\sqrt{m}$ . A weight  $\rho \sim 1/\sqrt{m}$  corresponds to a uniform distribution on this scale.

values of delta where  $\log L(\delta) = \log L_{max} - \frac{1}{2}$  and the two sigma range is limited by the values of delta where  $\log L(\delta) = \log L_{max} - 2$ .

We do this first in the range of masses where there exists a lower cutoff  $m_{low}$  which we take at 0.4 of the mass of the electron. In this case all powers of  $\delta$  are allowed in principle. We perform the analysis for only the quark masses and for the quark and lepton masses combined. The log likelihood function  $\log L(\delta)$  for the quarks and leptons combined is plotted in Fig. 4. In this case the favored value of  $\delta$  is almost exactly unity, with a range

$$\delta = 1.02 \pm 0.08. \quad (22)$$

If we only use the information in the quark masses we find nearly the identical result,  $\delta = 0.99 \pm 0.10$ . The error bars in these results include the effects of the limited statistics and get smaller when we include the lepton masses.

Alternatively we could consider power law weights that extend all the way down to  $m = 0$ . In this case the power  $\delta$  must be strictly less than unity. We obtain  $\delta = 0.86_{-0.05}^{+0.04}$  for quarks and leptons and  $\delta = 0.85_{-0.07}^{+0.05}$  for quarks only. All results from our likelihood fits are graphically summarized in Fig. 5.

Another way to probe the character of the weight is by a moment analysis. A random variable  $x$  which is uniformly distributed between 0 and 1 has moments

$$\langle x^n \rangle = \frac{1}{n+1}. \quad (23)$$

Of course for a small number of values drawn from a random distribution the moments will not be precisely these values, but will exhibit a scatter around these values due to the limited statistics. We can understand this effect by simulations. As an example we consider the second moment  $\langle x^2 \rangle$  of six random variables drawn from a uniform distribution from zero to one. We simulate six random numbers, evaluate  $\langle x^2 \rangle$  and repeat that many times. That results in a distribution of  $\langle x^2 \rangle$  which has the shape shown in Fig. 6. From this figure one can not only verify the expected average, but also understand the  $1\sigma$  and  $2\sigma$  ranges.

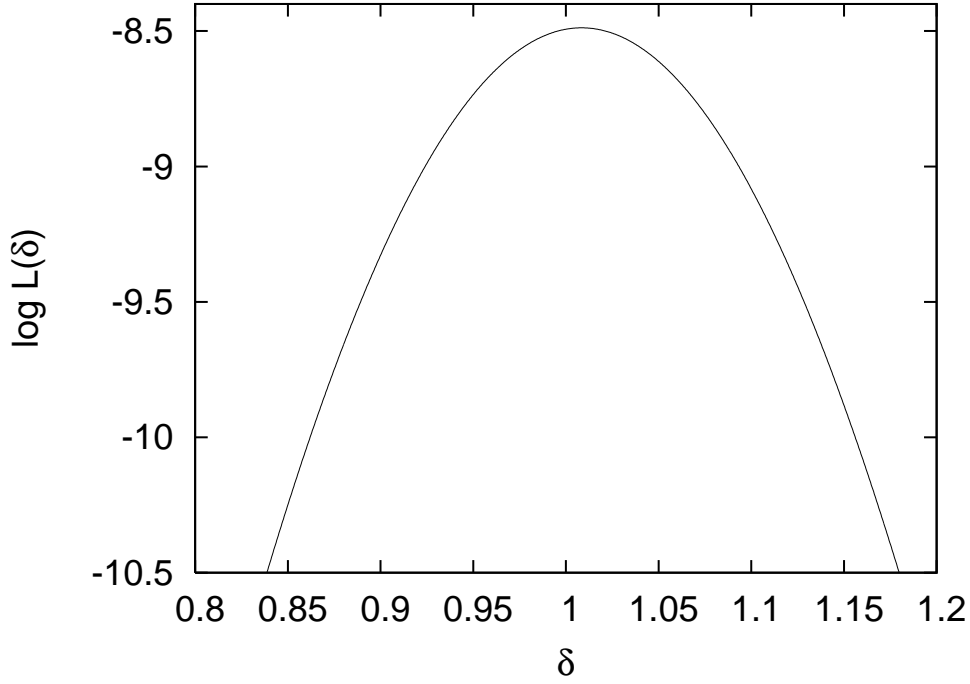


Figure 4: Log likelihood function for quark and lepton masses combined with  $m_{low}$ .

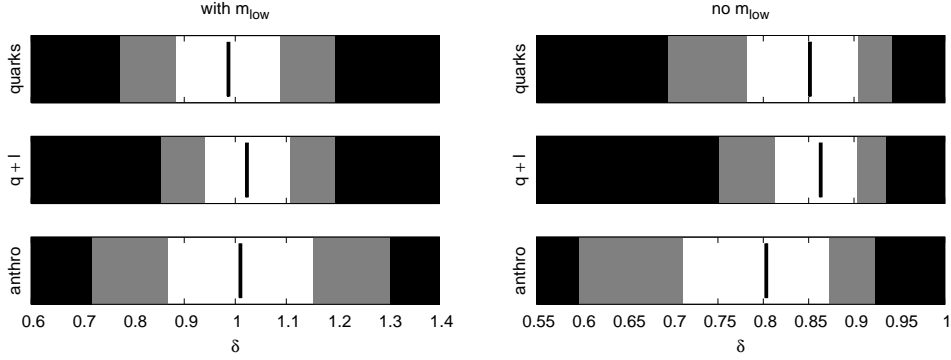


Figure 5: Results of the likelihood method. The black ranges are  $2\sigma$  excluded, the grey ones are  $1\sigma$  excluded and the lines inside the white regions are at the optimum powers  $\delta$ . The upper results are the ones taking only the quark masses into account, the ones in the middle are from quarks and leptons combined and the results at the bottom are the ones for quarks and leptons with anthropic constraints.

For example, at two standard deviations we find the allowed range of the second moment of six randomly selected numbers is

$$0.112 \leq \langle x^2 \rangle \leq 0.585. \quad (24)$$

We apply these tests to the weights, asking if the masses at  $M_W$  correspond to a uniformly distributed random variable in  $m^{1-\delta}$  or  $\log m$ . We use the first three moments  $n = 1, 2, 3$  and require that all of these moments fall within the  $1\sigma$  or  $2\sigma$  ranges. Besides the moments  $\langle x^n \rangle$ , we also take into account  $\langle (1-x)^n \rangle$  and  $\langle (\frac{1}{2}-x)^n \rangle$  for  $n = 1, 2, 3$

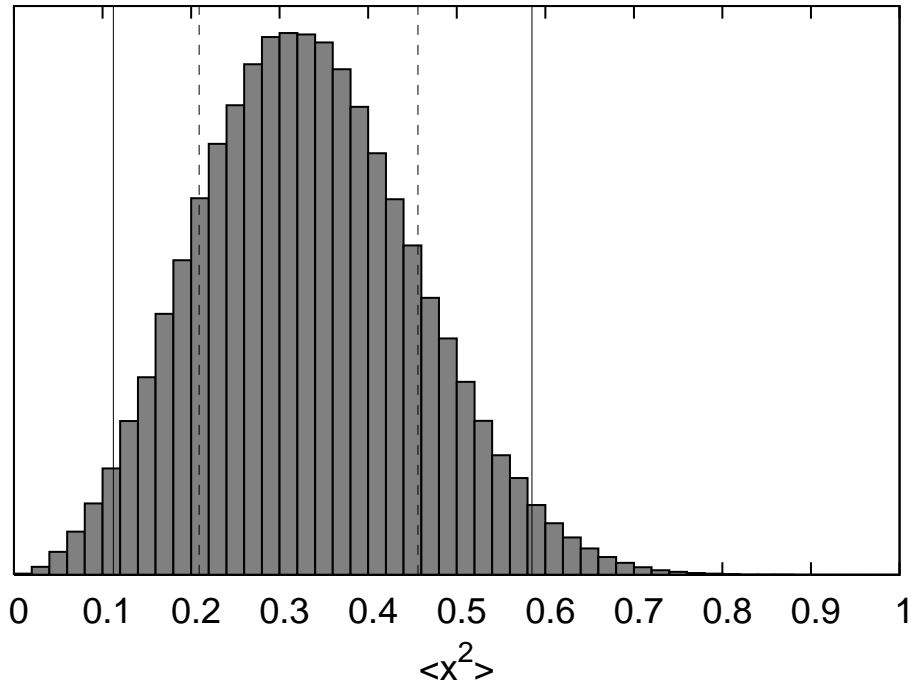


Figure 6: Distribution of  $\langle x^2 \rangle$  for six random variables. The dashed lines mark the  $1\sigma$  ranges and the solid lines mark the  $2\sigma$  ranges.

and always take the most stringent bounds of all of them. The results from this moment analysis are plotted in Fig. 7.

Comparing with the  $1\sigma$  and  $2\sigma$  ranges from the likelihood method, we find that the allowed ranges are somewhat smaller from the moments analysis but otherwise are in good agreement. The fact that we always take the most stringent bounds in the moment analysis probably lets the allowed ranges shrink in comparison to the ones from the likelihood method.

One subtlety we did not discuss so far is the distortion of our analysis by possible anthropic constraints. This is a difficult subject and we cannot fully address it here. However, anthropic issues have the potential to undermine our fundamental assumption that the masses which we see are representative of the Standard Model ensemble. This is because the formation of complex elements which are necessary for life can only occur for certain configurations of the charged fermion masses. In particular some masses need to be light [6, 7, 8] on the QCD scale - otherwise the nucleons would decay rather than be bound in the nucleus. Thus the masses that we see may represent an anthropic bias in favor of light masses.

We can partially address anthropic issues by the following strategy. We will eliminate from consideration the up and down quarks and the electron, and will revisit our analysis only considering the second and third generations of fermions. This is because the first generation masses may be biased by anthropic considerations while there are no known anthropic constraints on the heavier fermions.

Specifically, we proceed as follows. We drop the light masses  $m_u$ ,  $m_d$  and  $m_e$  from our analysis. We also exclude the possibility that more than these three fermions are very light. This is not a firm requirement as there could be different pattern of elements if more quarks

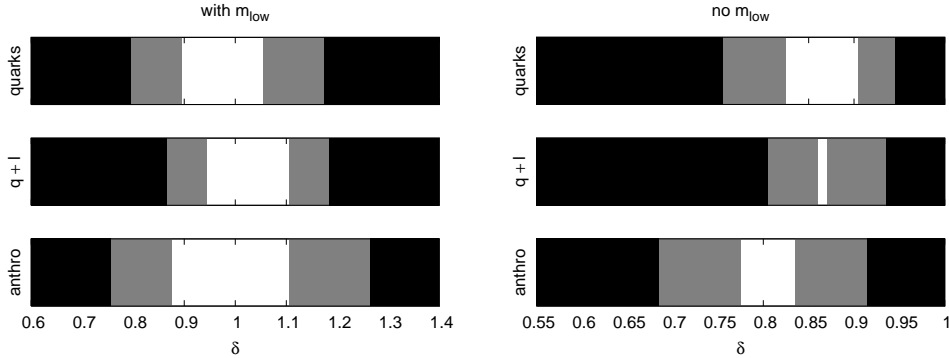


Figure 7: Results of the moment analysis. The black ranges are  $2\sigma$  excluded and the grey ones are  $1\sigma$  excluded. The upper results are the ones taking only the quark masses into account, the ones in the middle are from quarks and leptons combined and the results at the bottom are the ones for quarks and leptons with anthropic constraints.

or leptons were light. However, this assumption that only the three members of the first generation play a role in the elements does correspond to the anthropic setting that we find ourselves in, so it makes sense to study only this situation. We apply this constraint by not allowing any other masses to occur below 10 MeV. This boundary is chosen because of the nuclear binding energy of 10 MeV/nucleon. Fermions with masses greater than this do not play a role in nuclear binding because they decay weakly rather than being stable in the nucleus. For distributions with a low mass cutoff, we accomplish this by taking  $m_{low} = 10$  MeV.

The results from our likelihood and moment analysis with anthropic considerations are included in Fig. 5 and 7. It is interesting that this modification does not significantly change our results. For weights with a lower bound  $m_{low}$  on the masses all results are consistent with a scale invariant weight  $\delta = 1$ . For the weights extending all the way down to  $m = 0$ , a power  $\delta$  in the range  $\delta = 0.7 - 0.9$  seems preferred. One can understand why there is little change in our results by looking at the visual representation of the distribution in Fig. 1. Our procedure for simulating anthropic constraints consists of dropping the three lowest masses and applying a cutoff at 10 MeV, which on this figure is just above the mass of the down quark. One can see that the remaining 4 quark and 2 lepton masses are consistent with uniform distribution by themselves. Thus we have evidence for the scale invariant form even considering only the heavier masses for which there is no known anthropic constraints.

Finally, let us now consider the effect of scaling the quark and lepton masses up to the GUT scale (taken to be  $10^{16}$  GeV). We could equivalently scale down a distribution from the GUT scale and apply separate weights for quarks and leptons, as illustrated in Section 2. However, it is simpler to use the renormalization group to scale the masses up and study a common distribution at the GUT scale. This explores the issue of whether the quarks and leptons should be combined using the same distribution at the  $W$  scale or at the GUT scale. We will see that there is very little difference between these alternatives. The renormalization group equations were given in the previous section. We use only the Standard Model interactions in the running of the masses up to the GUT scale. The resulting Yukawa couplings defined at  $10^{16}$  GeV are given in Table 3.

Again we can visually explore the the comparison of these results with the scale invariant weight by displaying them on a log scale, as in Fig. 8. While there is a small shift in the

$h_u$	$h_d$	$h_s$	$h_c$	$h_b$	$h_t$
$0.46 \times 10^{-5}$	$0.92 \times 10^{-5}$	$1.7 \times 10^{-4}$	$1.7 \times 10^{-3}$	$6.5 \times 10^{-3}$	0.63
		$h_e$	$h_\mu$	$t_\tau$	
		$2.9 \times 10^{-6}$	$6.1 \times 10^{-4}$	0.01	

Table 3: Quark and lepton Yukawa couplings at the scale  $M_{GUT} = 10^{16}$  GeV.

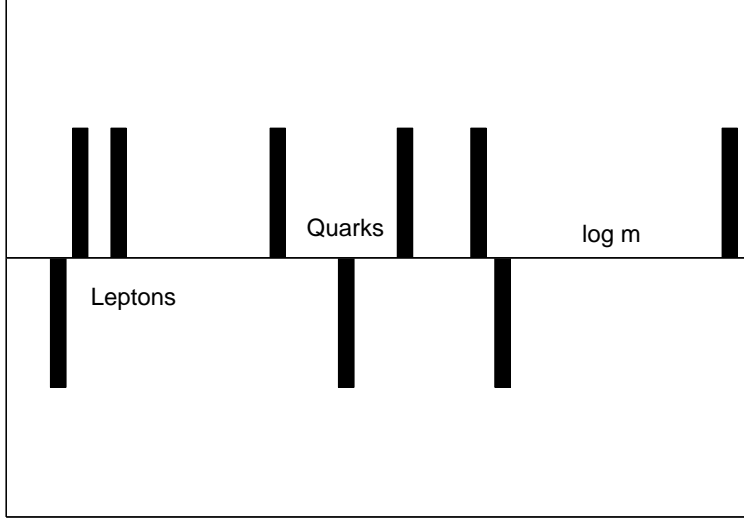


Figure 8: Quark and lepton Yukawa couplings, defined at the GUT scale  $\mu = 10^{16}$  GeV, on a logarithmic scale. This differs from Fig. 1 by the (different) renormalization of the quark and lepton couplings as one transforms them to the GUT scale.

relative placement of the quarks and leptons, due to their different running up to the GUT scale, this make no qualitative difference in the apparent randomness of the distribution. This is also manifest in a maximum likelihood fit. We consider the weights with both upper and lower cutoffs - in particular we use  $h_+ = 1$  and  $h_- = 1.2 \times 10^{-6}$ . As noted previously, these correspond to a maximum quark mass of 197 GeV and a minimum lepton mass of 0.20 MeV. A maximum likelihood analysis of the weight for the combined quark and lepton Yukawa coupling as a function of  $\delta$  again favors values of  $\delta$  near one with a fit value of  $\delta = 1.06 \pm 0.08$ . The  $2\sigma$  allowed range of  $\delta$  is  $0.89 - 1.24$ . These ranges are very similar to the ones that we obtained when we simply combined quark and lepton masses at the  $W$  scale. We conclude from this that effects of different treatments of quarks and leptons are small. Also we have learned that it does not make any practical difference if we determine the weight at the  $W$  scale or at the GUT scale - the distribution is close to scale invariant at either energy.

## 4 Quark mixing

In this section we extend our discussion to the full Yukawa matrices for up- and down-type quarks, generating not only the quark masses but also the CKM mixing elements. Again, the assumption is that each of the Yukawa elements can be treated as an independent variable

to be generated independently from a probability distribution function. Of course, even in the landscape, this assumption could be incorrect if there are symmetries or dynamics that constrain the independent variables in the Yukawa matrices. However, we will see that this ansatz does statistically account for the hierarchy that we see in the CKM elements. The reason this occurs is simple - because the weight is peaked at low mass, many of the Yukawa couplings are small and therefore generate small mixing angles. This dominance of small Yukawa elements may also provide an approximate explanation for the idea of “textures” in the quark mass matrices [11].

The generation of the quark mass matrices is a well-known procedure in the Standard Model [9]. The mass matrix for the up-type quarks, for example, follows from the Yukawa coupling to the Higgs through the relation

$$M_{0ij}^{(u)} = \frac{h_{ij}}{\sqrt{2}}v \quad (25)$$

where  $h_{ij}$  are the Yukawa couplings. This consists of 9 independent complex elements. The diagonalization of this matrix occurs through separate transformations on the left handed and right handed quarks

$$m^{(u)} = \begin{pmatrix} m_u & 0 & 0 \\ 0 & m_c & 0 \\ 0 & 0 & m_t \end{pmatrix} = V_L^{(u)\dagger} M_0^{(u)} V_R^{(u)}. \quad (26)$$

A similar process occurs for the down-type quarks

$$m^{(d)} = \begin{pmatrix} m_d & 0 & 0 \\ 0 & m_s & 0 \\ 0 & 0 & m_b \end{pmatrix} = V_L^{(d)\dagger} M_0^{(d)} V_R^{(d)}. \quad (27)$$

The CKM matrix is then formed by the product of the two left handed rotation matrices

$$V_{CKM} = V_L^{(u)\dagger} V_L^{(d)}. \quad (28)$$

In general the elements of the mass matrix  $M_{0ij}$  are complex-valued. In our model the magnitude of the elements of  $M_{0ij}$  are being distributed from  $m_{low}$  to  $m_*$  according to the weight  $1/m^\delta$ . We take the phases of the elements of  $M_{0ij}$  to be uniformly distributed between 0 and  $2\pi$ . The appearance of complex elements for  $M_{0ij}$  is required for the existence of CP violation and of course is not forbidden by any of the symmetries of the Standard Model. However, we have also simulated the mixing matrices with real elements and we note that this does not change any of our qualitative results, aside of course from the measure of CP violation.

A first question to be addressed is whether an assumed weight for the Yukawa couplings will lead to the same weight being applicable for the masses that emerge as output from the diagonalization process. We cannot address this question analytically, so we approach it via simulations. The result that we find is that there is a change in the weight between the initial Yukawa couplings and the final masses and that this change is roughly categorized by a shift in the power  $\delta$  by about  $-0.16$ .

In order to demonstrate this, we have generated a large sample of mass matrices of Yukawa couplings with a scale invariant weight  $\rho \sim 1/h$ , diagonalized the matrices and bin and plot the resulting mass values on a logarithmic scale in Fig. 9 (a). If the resulting

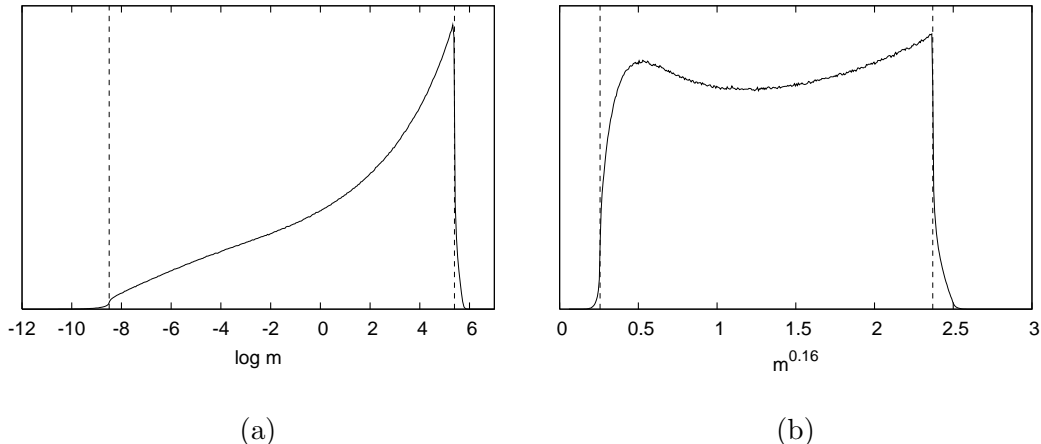


Figure 9: Elements of mass matrices have been distributed according to the scale invariant weight. In (a) we bin and plot the the eigenvalues of the mass matrices on a logarithmic scale, whereas in (b) we do the same on an  $m^{0.16}$  scale. The vertical dashed lines indicate the values of  $m_{low}$  and  $m_*$ .

distribution was also scale invariant, this plot would be flat. However, the result is not flat. However, when plotted versus  $m^{0.16}$  in Fig. 9 (b), we see that the resulting distribution is almost flat, indicating that the result is compatible with a weight of  $\rho \sim 1/m^{0.84}$ . Likewise if we simulate a weight for the Yukawa interactions of  $\rho \sim 1/h^{1.16}$  and bin and plot the resulting masses on a logarithmic scale in Fig. 10 we see an almost flat distribution which would correspond to a scale invariant weight for the output masses.

Another outcome we see is that after the diagonalization of the Yukawa matrices the limits  $m_{low}$  and  $m_*$  are washed out for the mass eigenvalues. There are masses smaller than  $m_{low}$  and larger than  $m_*$ , but as one can see in Fig. 9 and 10 masses which are orders of magnitude smaller than  $m_{low}$  or larger than  $m_*$  are highly suppressed.

A weight for the Yukawa matrix elements that is capable of explaining the observed quark masses must therefore have a higher power  $\delta$  than what we found in our analysis in Section 3. As we saw,  $\delta = 1.16$  for the Yukawa matrix elements roughly corresponds to a scale invariant distribution for the masses. The previous limits  $m_{low}$  and  $m_*$  can also be used for the Yukawa matrix elements.

Now we turn to the details of the simulation of the CKM matrices. First, we generate a large sample of mass matrices for both up-type quarks and down-type quarks. Each element of a particular mass matrix is taken to be independent of each other. By convention the largest masses in the two mass matrices are the top and the bottom, so we use the freedom to relabel the fields in order to place the largest element in the (3,3) position of the mass matrices.

As discussed above, the diagonalization of the mass matrices is being done by biunitary transformations. In general, in this procedure the physical mass eigenvalues of quarks have no constraint to fall within any particular range. However for this mixing analysis we wish to consider only output masses that are somewhat similar to those observed in nature. We impose this by considering only those mass matrices for which mass eigenvalues for up and down quarks (*i.e* the lightest eigenvalues of each matrix) are less than 10 MeV, mass eigenvalues for charm and strange quarks are within 50 MeV and 2 GeV and mass

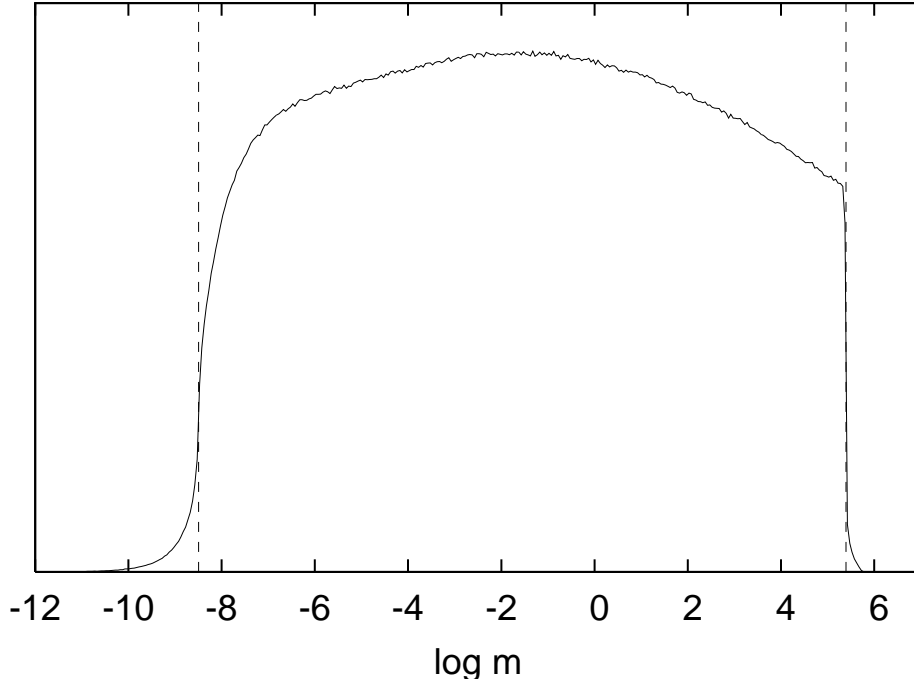


Figure 10: Distribution of the eigenvalues of the mass matrices, on a logarithmic scale, when the elements of the mass matrices have been distributed according to weight  $\rho \sim 1/m^{1.16}$ .

eigenvalues for top and bottom quarks are greater than 3 GeV.

We construct CKM elements from two left handed rotation matrices, one from up-type quarks and the other from the down-type quarks. In the results, there are a few discrete classes for the pattern of mixing angles. Since we have not imposed the generation structure, there is a set of cases where the up and the strange are dominantly coupled to each other and  $V_{ud}$  is small. Likewise there is a small number of cases where the charm and bottom quarks are dominantly coupled to each other. We discard these cases and only consider those results which exhibit the proper generation structure such that the largest couplings are to members of the same generation (as defined by the relative masses).

We use a weight for the Yukawa couplings of  $1/h^{1.16}$ , which generates the almost scale invariant weight for the masses. With these constraints, the resulting distribution of the magnitude of the  $V_{us}$  elements of CKM matrices is shown in Fig. 11. One can see that the distribution is peaked at lower values. When one looks more closely at the distribution of  $V_{us}$  at very low values, one sees that the peak is located at about 0.002.<sup>1</sup> Another feature of the distribution is that it vanishes for values larger than  $1/\sqrt{2}$ . The reason for that is the generation structure we impose where we require the diagonal elements to be the largest elements in their row and column in the CKM matrix.

<sup>1</sup>When doing the same simulations without  $m_{low}$  this peak does not occur but the distribution for  $V_{us}$  reaches a maximum at zero. One can understand that from dimensional analysis: in the simulations with  $m_{low}$  there are two dimensionful parameters involved,  $m_*$  and  $m_{low}$  where  $m_{low}/m_* \ll 1$ . However, in the case without  $m_{low}$  there is only one dimensionful parameter. Therefore a peak for a dimensionless quantity such as  $V_{us}$  is expected to be found either at zero or at a value of order one in a case where only one dimensionful parameter exists.

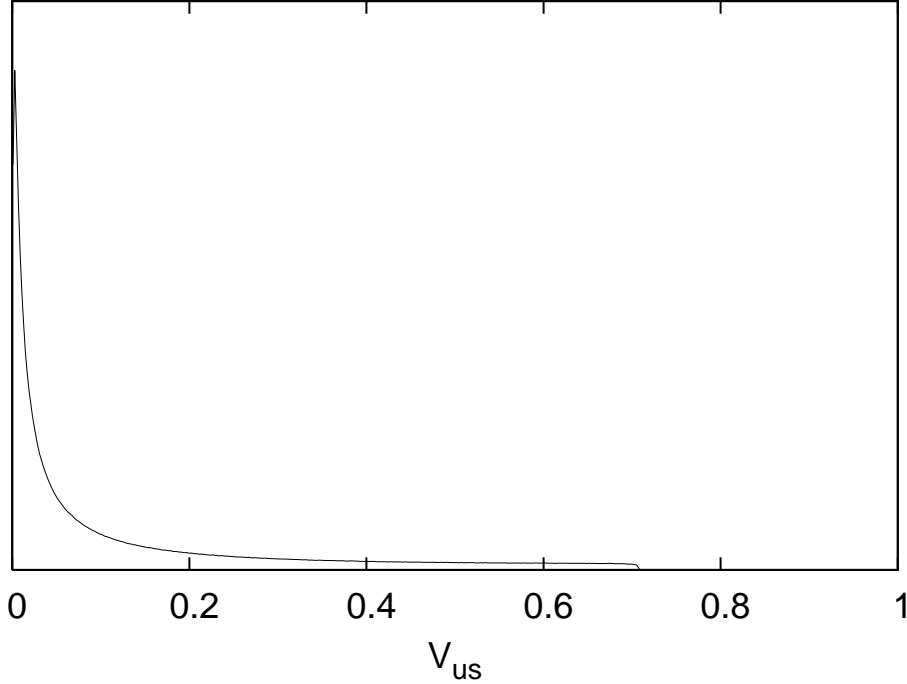


Figure 11: Distribution of the simulated values of  $V_{us}$ .

The other CKM elements we consider are  $V_{ub}$  and  $V_{cb}$ . For both we observe shapes of their distributions similar to the one for  $V_{us}$  as seen in Fig. 11, but with a higher preference for small values.

For the distributions of the CKM elements one cannot define  $1\sigma$  and  $2\sigma$  ranges as for Gaussian distributions since the peaks are very close to zero but the tails of the distributions are extremely long. Therefore we instead consider the medians of the distributions and the values where 68% and 95% of the elements lie below them. We call the ranges up to these values the  $1\sigma$  and  $2\sigma$  ranges respectively. For  $\delta = 1.16$  the observed values of  $V_{ub}$  and  $V_{cb}$  fall within the  $1\sigma$  ranges and the physical value for  $V_{us}$  is within the  $2\sigma$  range.

The medians of the CKM elements follow the similar hierarchy that is observed in nature. In Fig. 12 we plot the medians of  $V_{ub}, V_{cb}, V_{us}$  as a function of  $\delta$ . In general, there is a hierarchy in the magnitudes of the elements. This is understandable from the diagonalization procedure. Because of the  $1/h^\delta$  distribution, most Yukawa couplings are small. The mixing angles needed to diagonalize the mass matrices are proportional to the off-diagonal elements divided by the difference in masses. The mixing involving heavy top and bottom quarks will be smaller than those that involve the mixing of down and strange quarks. Thus we see that our model can accommodate the hierarchical structure of CKM elements.

After absorbing several complex phases into the definition of the quark fields, the CKM matrix can be expressed by four parameters, of which three are mixing angles and one is a complex phase. This complex phase indicates the existence of CP violation in the theory. Perhaps the best way to describe CP violation is through the ‘‘Jarlskog invariant’’,  $J$  [12] which is invariant under rephasing of the quark fields. All CP violation is proportional to

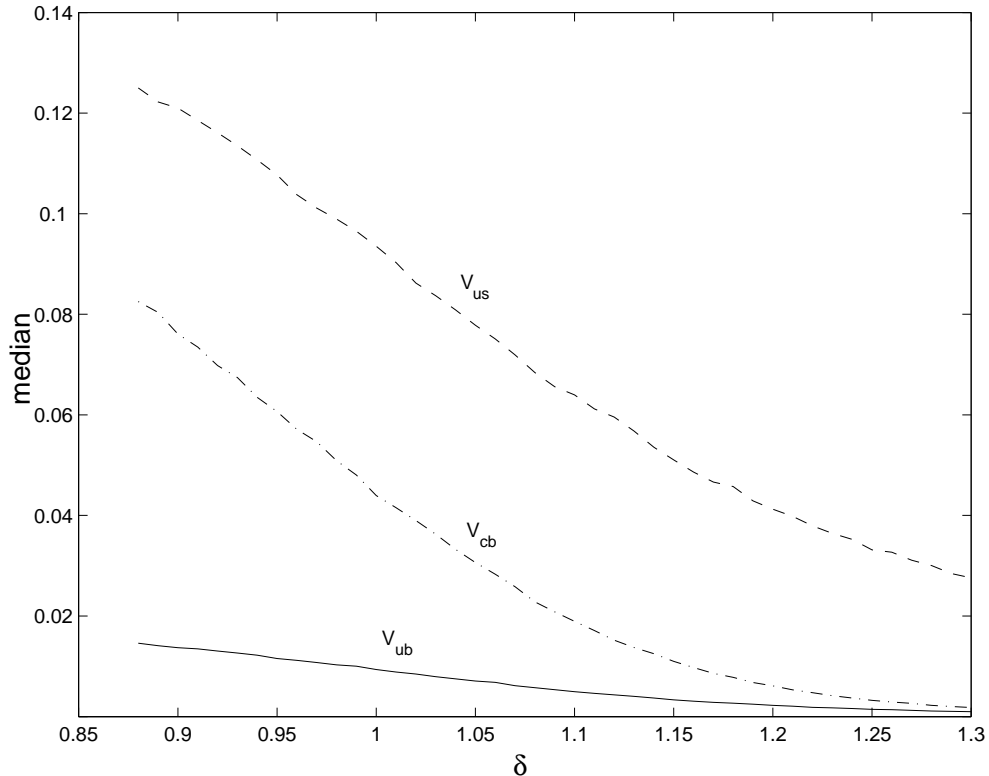


Figure 12: Medians of the CKM elements as a function of  $\delta$

the product of CKM elements

$$J = \text{Im}(V_{ud}V_{cs}V_{us}^*V_{cd}^*). \quad (29)$$

In nature, this is observed to have the value  $J = (2.88 \pm 0.33) \times 10^{-5}$  [10]. In Fig. 13 we plot the distribution of  $J$  and indicate the  $1\sigma$  range. We note that observed value of  $J$  in nature is well within the  $1\sigma$  range. We conclude that, within the hypothesis of the weight, the observed magnitude of CP violation is quite natural for the same probability distributions that describe the quark masses.

## 5 Neutrino masses and mixing

The neutrino masses are different enough from those of the other fermions that it is clear that they should not be governed by the same weight. Moreover, there are strong theoretical reasons why neutrino masses should be treated differently. In this section we explore the description of the neutrino masses and mixing in the case where they are described by the Type I seesaw mechanism [13]. Specifically we will assume that the Dirac component of neutrino masses is governed by the same weight as the charged leptons, and will add the possibility of a different weight for the Majorana component of the mass. Unfortunately our exploration will be somewhat inconclusive. The observed pattern of masses and mixings is not highly typical of the theoretical distributions, but it is also not statistically excluded

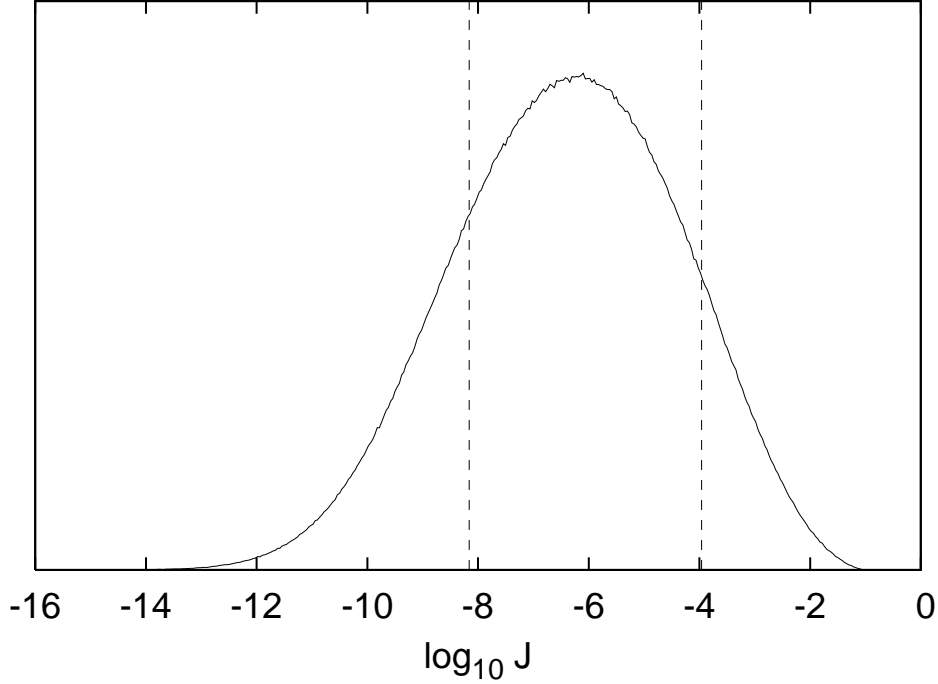


Figure 13: The Jarlskog invariant for quarks describing the magnitude of CP violation

at the  $2\sigma$  level. We note that other attempts at simulating neutrino properties with a statistical distribution can be found in [18] and [19]. We compare our analysis to these at the end of this section.

Our present knowledge of neutrino masses comes from various neutrino oscillation experiments and from the measurements of the anisotropies in the CMB by WMAP and large scale structure formation. From neutrino oscillation experiments, we know two mass differences and WMAP gives an upper bound on the sum of the neutrino masses [14, 15]:

$$5.4 \times 10^{-5} \text{ eV}^2 \leq \Delta m_{12}^2 \leq 9.5 \times 10^{-5} \text{ eV}^2$$

$$1.2 \times 10^{-3} \text{ eV}^2 \leq |\Delta m_{13}^2| \leq 4.8 \times 10^{-3} \text{ eV}^2$$

$$\sum_k m_k \leq 0.7 \text{ eV} \tag{30}$$

First we consider the neutrino masses by themselves without mixing. In the Type I seesaw mechanism, the light neutrino masses  $m_i$  are of the form

$$m_i = \frac{m_{D,i}^2}{M_M} \tag{31}$$

where  $m_{D,i}$  are the Dirac masses connecting left and right handed fields and  $M_M$  is the Majorana mass term of the right handed neutrinos.

We assume that the Dirac masses come from the same weight as the quark and charged lepton masses  $\rho \sim 1/m^\delta$  and that the Majorana mass  $M_M$  is a common scale. Since in

the Type I seesaw, the Dirac masses are proportional to the Higgs vev, it is a reasonable assumption that the weight is the same as that for the quarks and charged leptons. Note that a scale invariant weight for the Dirac masses predicts that the neutrinos will also be distributed with a scale invariant weight. If the Dirac masses are distributed with a weight  $\sim 1/m^\delta$ , and the Majorana mass is taken as a constant, then the neutrino masses are distributed with a weight

$$\rho_\nu(m_\nu) \sim \frac{1}{m_\nu^{\delta_\nu}} \sim \frac{1}{m_\nu^{2\delta-1}} \quad (32)$$

and the use of  $\delta = 1$  implies  $\delta_\nu = 1$  also.

An initial result is that this scheme greatly favors a “normal” hierarchy in the neutrino masses with  $m_1 \ll m_2 \ll m_3$ . In this case the solar mass difference is representative of the mass scale of the second lightest neutrino with mass  $m_2$ . The third neutrino is then heavier, with a mass  $m_3$  of order the atmospheric mass difference. The scale invariant weight favors this because it favors small masses. It would be unlikely that there are two large masses that just happened to be so close together to yield the small solar mass difference. In the simulations that we describe below for the case involving mixing, the probability of obtaining the mass differences with an inverted hierarchy compared to a normal hierarchy was about 0.1%. A quasi degenerate neutrino mass spectrum is even much more unlikely. From now on we will assume that a “normal” hierarchy exists.

One might hope that the observed masses, combined with the assumption that the Dirac masses contribute to the seesaw mechanism with the weight determined for the other fermions, would lead to a prediction for the scale of the Majorana mass. In practice this does not occur. We have performed a likelihood fit for the scale of the Majorana mass  $M_M$  and we find that the  $2\sigma$  allowed range for  $M_M$  spans from  $10^5$  GeV to  $10^{15}$  GeV. The details of this fit are given in the Appendix.

One way to see why the limits on the Majorana mass scale are that weak is to plot the masses on a log scale. Of course we do not know the absolute masses precisely since we have only the mass differences. However, under the assumption of a normal hierarchy we know the largest mass quite well and, if the lightest mass is not anomalously close to the second lightest mass, we have a reasonable estimate of the second lightest mass. However, there is no constraint at all on the mass of the lightest neutrino. Thus the situation is close to that pictured in Fig. 14, where the rough positions of the two heaviest neutrinos are pictured and the lightest is allowed at almost any location smaller than these on the logarithmic scale.

In the figure also are shown the ranges allowed for the neutrino masses in the situation where the Dirac mass is described by the scale invariant weight and the Majorana mass scale  $M_M$  is a constant. The ranges are shown for various values of the Majorana mass scale  $M_M$ . The scale invariant distribution would correspond to a uniform random distribution on this logarithmic scale. It is clear visibly that if we allow the lightest neutrino mass to be in a broad possible range, that a wide range of Majorana masses is consistent with the scale invariant mass distribution. For high Majorana scales  $M_M$  there is however more “phase space” for the lightest mass which leads to the slight preference for high Majorana mass scales  $M_M$  as seen in our likelihood fit. Independent of the scale  $M_M$  one can see that the two heaviest neutrino masses are always very close together on a logarithmic scale. We have to consider that a statistical accident in our scheme.

The analysis of neutrino mixing angles also is not very definitive. Neutrino mixing is somewhat different than quark mixing. Let us review the experimental data and the mixing formalism within the context of the seesaw mechanism [16].

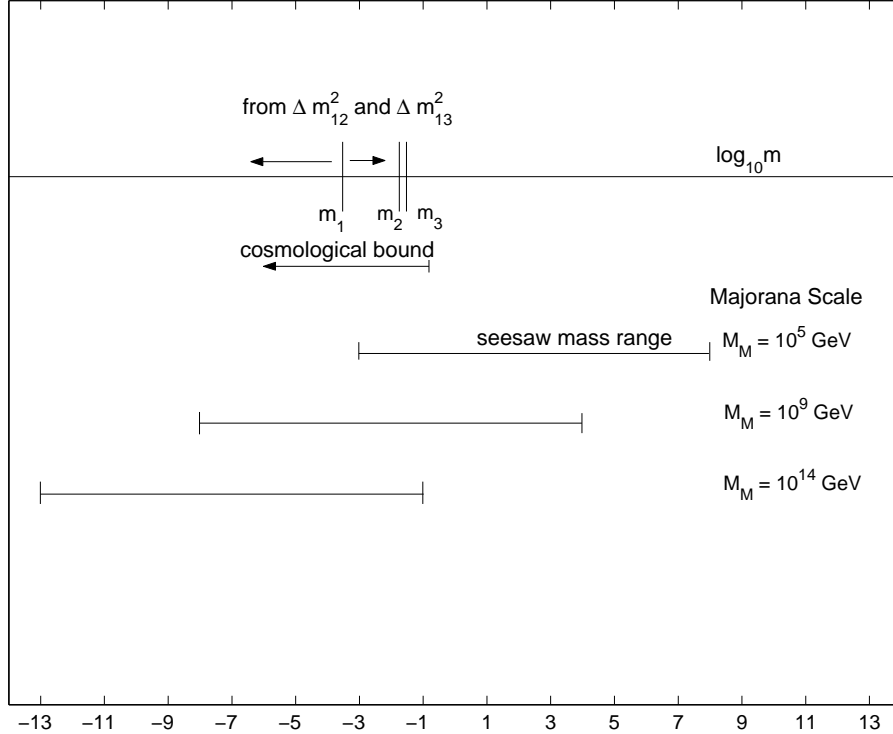


Figure 14: The neutrino masses on a logarithmic scale. The mass differences were translated into rough mass estimates as described in the text. Note that the lightest mass is unconstrained at small values of the mass. If the distribution is to be described by a scale invariant weight, these masses should be uniformly distributed on this log scale. The range of the distribution is also shown for various values of the Majorana mass. Given the limited statistics, it is hard to determine if a scale invariant distribution is appropriate or to bound the Majorana mass scale.

The lepton equivalent of the CKM matrix is called the MNS matrix. We can parameterize the MNS matrix in the form [10]

$$V_{MNS} = \begin{pmatrix} c_{12}c_{13} & s_{12}c_{13} & s_{13}e^{-i\delta} \\ -s_{12}c_{23} - c_{12}s_{23}s_{13}e^{i\delta} & c_{12}c_{23} - s_{12}s_{23}s_{13}e^{i\delta} & s_{23}c_{13} \\ s_{12}s_{23} - c_{12}c_{23}s_{13}e^{i\delta} & -c_{12}s_{23} - s_{12}c_{23}s_{13}e^{i\delta} & c_{23}c_{13} \end{pmatrix} \times \text{diag}(e^{i\alpha_1/2}, e^{i\alpha_2/2}, 1) \quad (33)$$

where  $c_{ij} \equiv \cos \theta_{ij}$  and  $s_{ij} \equiv \sin \theta_{ij}$ . The three  $\theta_{ij}$ 's are mixing angles and  $\delta, \alpha_1, \alpha_2$  are CP violating phases. The phases  $\alpha_i$  are only observable if neutrinos are Majorana particles. The present  $3\sigma$  allowed ranges for the mixing angles are [14, 17]

$$\begin{aligned} \sin^2 2\theta_{23} &\geq 0.92 \\ 0.70 &\leq \sin^2 2\theta_{12} \leq 0.95 \\ \sin^2 \theta_{13} &\leq 0.048. \end{aligned} \quad (34)$$

and nothing is known so far about the CP violating phases. The existence of the two large mixing angles  $\theta_{12}$  and  $\theta_{23}$  is the most striking difference between the MNS and the CKM matrix.

Both the mass matrices for charged leptons and for neutrino have to be diagonalized and their lefthanded unitary rotation matrices give rise to the MNS matrix. For the charged leptons the diagonalization procedure is analogous to the ones for the quarks:

$$m^{(l)} = \begin{pmatrix} m_e & 0 & 0 \\ 0 & m_\mu & 0 \\ 0 & 0 & m_\tau \end{pmatrix} = V_L^{(l)\dagger} M_0^{(l)} V_R^{(l)} \quad (35)$$

After the seesaw mechanism the neutrino mass matrix is

$$M_0^{(Seesaw)} = M_0^{(D)} \frac{1}{M_0^{(Major)}} M_0^{(D)T} \quad (36)$$

where all ingredients are  $3 \times 3$  matrices. Note that  $M_0^{(Major)}$  has to be symmetric. The Dirac part is diagonalized as follows:

$$m^{(D)} = \begin{pmatrix} m_{D,1} & 0 & 0 \\ 0 & m_{D,2} & 0 \\ 0 & 0 & m_{D,3} \end{pmatrix} = V_L^{(D)\dagger} M_0^{(D)} V_R^{(D)} \quad (37)$$

Plugging the diagonalization of the Dirac part into Eq. (36) yields

$$M_0^{(Seesaw)} = V_L^{(D)} \mathcal{C} V_L^{(D)T} \quad (38)$$

where the central matrix  $\mathcal{C}$  is defined as

$$\mathcal{C} = m^{(D)} V_R^{(D)\dagger} \frac{1}{M_0^{(Major)}} V_R^{(D)*} m^{(D)}. \quad (39)$$

The central matrix  $\mathcal{C}$  is diagonalized with a unitary matrix  $\mathcal{F}$ :

$$\mathcal{C} = \mathcal{F} m_\nu \mathcal{F}^T = \mathcal{F} \begin{pmatrix} m_1 & 0 & 0 \\ 0 & m_2 & 0 \\ 0 & 0 & m_3 \end{pmatrix} \mathcal{F}^T \quad (40)$$

The masses in the diagonal matrix  $m_\nu$  are the physical neutrino masses.

The MNS matrix involves the rotations that diagonalize the mass matrices of the charged leptons and the neutrinos. This also includes the rotation that diagonalizes the central matrix. Therefore, in terms of the quantities defined above, the MNS matrix becomes

$$V_{MNS} = V_L^{(l)\dagger} V_L^{(D)} \mathcal{F}. \quad (41)$$

One might hope that the striking features of the neutrino mixing matrix might allow us to gain some insight into the Majorana sector of the theory, which comes from very high scale physics and for which we cannot argue for any preferred weight. Unfortunately this does not happen. We have simulated the neutrino mixing by considering a variety of possibilities for the Majorana mass matrix. We have allowed for different power law weights for the Majorana mass matrix as well as flat distributions or even a common mass. In each case we took the Dirac Yukawa couplings to be distributed with the weight  $\sim 1/m^{1.16}$ . The

results for the mixing angles in each case were so similar that we do not bother to display the differences. In each case, the mixing angles were dominated by small mixings, as we also found for the CKM mixing angles.

The reason for that is that the only difference within our scheme between the CKM and the MNS matrix is the additional factor of the rotation matrix  $\mathcal{F}$  that contributes to the MNS matrix.  $\mathcal{F}$  diagonalizes the central matrix  $\mathcal{C}$  from Eq. (39) that contains two factors of  $m^{(D)}$ . Since the diagonal Dirac mass matrices  $m^{(D)}$  come from a distribution  $\rho \sim 1/m^\delta$  we usually expect the entries of  $m^{(D)}$  to have a hierarchical pattern with  $m_{D,1} \ll m_{D,2} \ll m_{D,3}$ . In order to obtain large mixing angles from  $\mathcal{F}$  some of the entries in the central matrix  $\mathcal{C}$  must be of the same order. That however can only be achieved through a numerical coincidence or a correlated hierarchy of  $M_0^{(Maj)}$  designed to counterbalance the hierarchy present in  $m^{(D)}$  [16]. Our random matrices  $M_0^{(Maj)}$  are always simulated independently from all Dirac mass terms and thus there is no correlated hierarchy and not many more cases of two large mixing angles than for the CKM matrix, no matter how we simulate the Majorana mass matrix.

From now on, we always use Majorana mass matrices with elements distributed uniformly between zero and a Majorana scale  $\Lambda_{Maj}$ . The charged lepton mass matrices and the Dirac mass matrices are simulated using a weight  $\rho \sim 1/m^{1.16}$ . The neutrino masses we get from these simulations are close to a scale invariant distribution similar to the case of the quarks as seen in Fig. 10 in Section 4.

We are interested in the probability of finding large mixing angles, especially the “two large mixing angle” solution found in nature, using the parameterization of Eq. (33). We will define a large mixing angle to be an angle between  $30^\circ$  and  $60^\circ$  which corresponds to  $\sin^2 2\theta > 0.75$ .

In studying the properties of neutrino mixing, we have run simulations under various conditions. In the first setting, we impose no constraints at all and compare the percentage of two large mixing angles between the CKM matrix and the MNS matrix. We find two large mixing angles in 5% of the simulations for the CKM matrix, whereas for MNS matrix the percentage is a little higher being 6.5%. This difference is due to the seesaw mechanism i.e. due the effect of  $\mathcal{F}$  matrix in Eq. (41). Note that the resulting distributions of mixing angles for the MNS matrix are independent of the Majorana scale when there are no constraints.

We also have run simulations with constraints on the charged lepton masses and the neutrino masses. For the charged lepton masses we adopt similar constraints as we did in the previous section for the quarks considering only those mass matrices for which the mass eigenvalues for the electron (*i.e* the lightest eigenvalue of the charged lepton matrix) are less than 5 MeV, the mass eigenvalues for the muon are within 25 MeV and 1 GeV and the mass eigenvalues for the tau are greater than 1.5 GeV. For the neutrino masses we explore two different kinds of conditions. In one set of constraints, we accept only those neutrino masses where the mass differences lie within the experimental  $3\sigma$  allowed ranges and the cosmological bound is satisfied. A second set of simulations only requires that the two heaviest masses lie in the two decade wide mass range  $0.001 \text{ eV} < m_2, m_3 < 0.1 \text{ eV}$  with a mass ratio  $m_3/m_2 < 10$ , where  $m_3$  and  $m_2$  are the heaviest and second heaviest neutrinos respectively. This is more general than the first set of neutrino mass constraints, but captures what could be important features of the physical masses. In both the constrained cases, the number of cases with two large mixing angles depends on the Majorana scale.

In Tables 4 and 5 we present the results for the simulations concerning the number of large mixing angles when the above constraints are imposed. We see that the probability of two large mixing angles is never dominant. However, this probability is not small either.

$\Lambda_{Maj}$ [GeV]	$10^{14}$	$10^{12}$	$10^{11}$	$10^9$	$10^7$
Zero LMA	63.1%	60.2%	57.6%	53.2%	40.3%
One LMA	31.0%	32.8%	34.0%	35.9%	40.7%
<b>Two LMA</b>	4.5%	5.4%	6.6%	8.7%	15.4%
Three LMA	1.5%	1.6%	1.8%	2.2%	3.7%

Table 4: Percentages of outcomes depending on the number of large mixing angles and the Majorana scale when the masses satisfy the  $3\sigma$  bounds for the neutrino mass differences and the cosmological bound.

$\Lambda_{Maj}$ [GeV]	$10^{14}$	$10^{12}$	$10^{11}$	$10^9$	$10^7$
Zero LMA	49.5%	47.8%	46.4%	42.4%	33.1%
One LMA	42.9%	43.2%	43.2%	43.4%	44.2%
<b>Two LMA</b>	5.8%	6.8%	8.0%	11.1%	17.7%
Three LMA	1.8%	2.2%	2.5%	3.0%	5.0%

Table 5: Percentages of outcomes depending on the number of large mixing angles and the Majorana scale when the masses  $m_2$  and  $m_3$  are in the range  $0.001 - 0.1$  eV with a mass ratio  $m_3/m_2 < 10$ .

Depending on the scenario considered and the Majorana scale, the percentage ranges from about 4% to 18% as we vary  $\Lambda_{Maj}$ . There is a general trend in the cases where constraints on the masses are imposed - the percentage is larger when the Majorana scale is smaller. This is readily understandable. When the Majorana scale is small, the average element in the mass matrix is comparable to or greater than the resulting mass eigenvalues, because in the seesaw mechanism the masses are proportional to  $1/\Lambda_{Maj}$ . When all elements are large, one requires larger mixing angles to diagonalize the mass matrix.

Our results are somewhat inconclusive. One finds solutions with two large mixing angles with a reasonable percentage. However, it is not the most likely outcome. Statistically, we can not conclude anything significant from a comparison with the observed mixing angles. This conclusion is independent of how we have modeled the possible randomness of the Majorana sector. We have also found that the information on the neutrino mass differences is unable to tightly constrain the scale of the Majorana sector.

We can also extract some predictive elements from our analysis. We will study these using a Majorana scale of  $\Lambda_{Maj} = 10^{12}$  GeV. In each case we also only consider those realistic solutions that satisfy the  $3\sigma$  bounds on the neutrino mass differences as well as the cosmological bound and that have large angles  $\theta_{12}$  and  $\theta_{23}$  and values of  $\theta_{13}$  smaller than the experimental bound, and thus are very similar to the real data.

Using these realistic simulations, we have studied the size of the third mixing angle  $\theta_{13}$ . The distribution of  $\sin\theta_{13}$  is shown in Fig. 15 within its  $3\sigma$  allowed range, that is for  $\sin^2\theta_{13} \leq 0.048$ . We see that the distribution of  $\sin\theta_{13}$  is not peaked at low values but rises towards its  $3\sigma$  upper bound, so that there is no reason to expect that the third mixing angle is suppressed. The median of the distribution is 0.14 and 95% of the values lie above 0.04.

We also have studied the neutrino equivalent of the Jarlskog invariant that signals the strength of CP violation for lepton number conserving processes the neutrino sector. This is plotted in Fig. 16. Here we see that the Jarlskog invariant is generally large, of order  $10^{-2}$ . We see that the peak of the distribution is close to its theoretical maximum possible

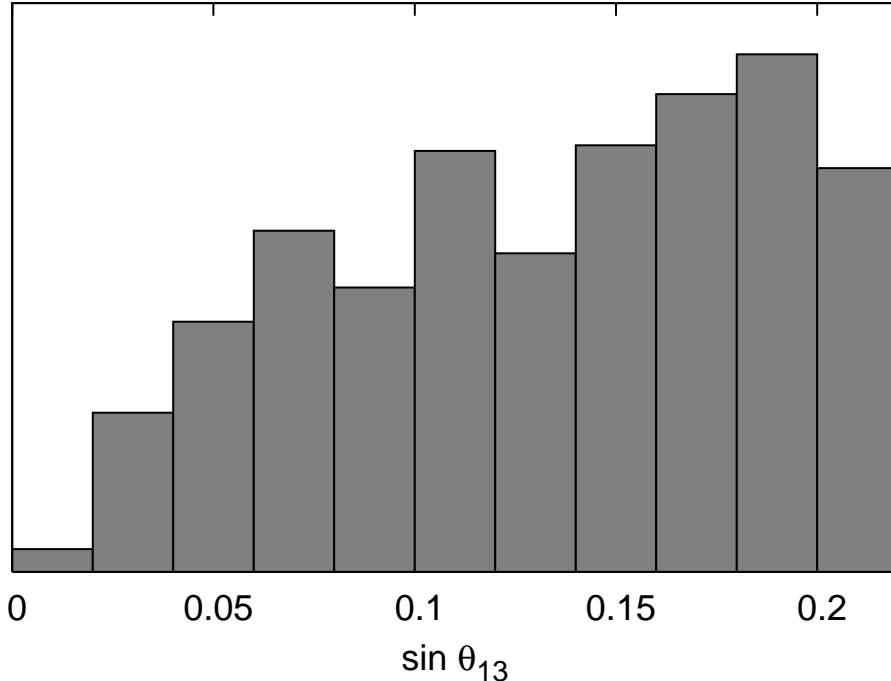


Figure 15: The distribution of  $\sin \theta_{13}$

value which is  $1/(6\sqrt{3})$ . The median of the distribution is at 0.016 and 95% of the values are above  $1.6 \times 10^{-3}$ .

Finally we consider the effective Majorana mass defined by

$$m_{ee} = \sum_i U_{ei}^2 m_i \quad (42)$$

which is the figure of merit in neutrinoless double beta decay [20]. The simulations of this parameter are shown in Fig. 17 again for the realistic case very similar to nature. We see that the distribution decreases approximately linearly until a value of 0.008 eV, with only very few values higher than that. These come from cases where the neutrino masses are not strictly hierarchical and the lightest mass is close to the second lightest mass. The median of the distribution is at 0.0028 eV, 95% are higher than  $3.5 \times 10^{-4}$  eV. 95% of the values lie below 0.0068 eV which is consistent with other results that expect the effective Majorana mass for the case of hierarchical neutrino masses to be smaller than 0.0064 eV [20].

A pioneering effort in simulating neutrino mixing angles randomly in the context of the seesaw mechanism was the work of Goldman and Stephenson in 1981 [18]. These authors randomly populated both the Dirac and Majorana mass matrices with a uniform distribution and found that the typical case involved angles of the same size as the Cabibbo angle. The intent was not to invoke a random dynamical framework but to argue that unless the initial Yukawa couplings were peculiar, that we should expect to find Cabibbo-like mixing angles. More recently, the idea has surfaced under the label of “anarchy” in the works of [19]. These authors build in more of what is now known about the neutrino mass spectrum and, although again one most typically finds Cabibbo-like angles, they point out that one finds two large mixing angles (defined as  $\sin^2 2\theta > 0.5$ ) in about 13% of the cases when simulated

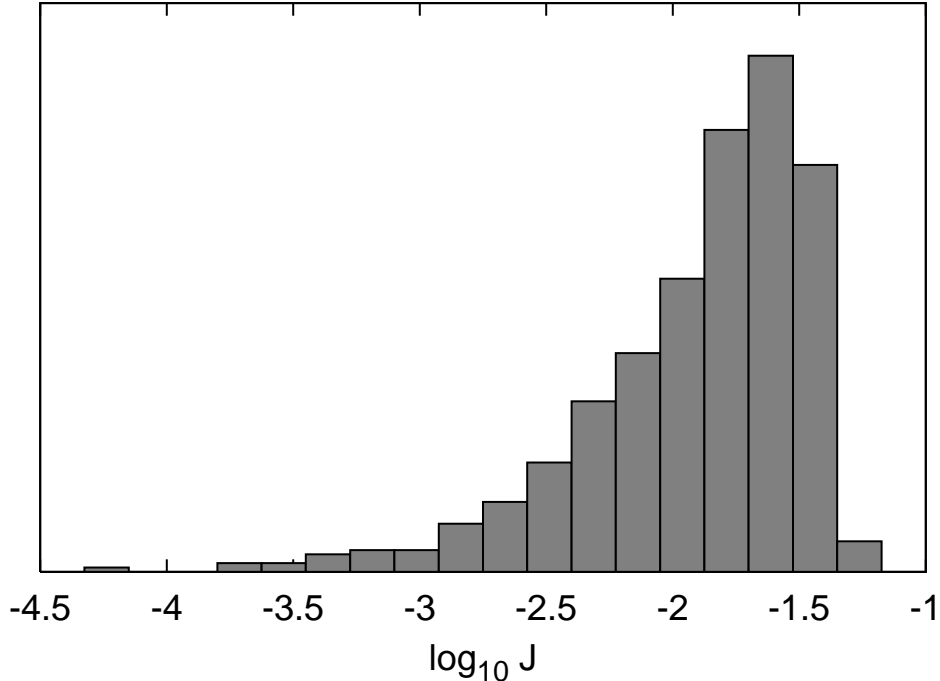


Figure 16: Distribution of the Jarlskog invariant  $J$  for neutrinos

with a uniform random distribution. Our considerations have been somewhat different. We have used the Dirac component of the neutrino masses to be the same distribution that has been used in the description of the charged leptons and the quarks, and considered various possibilities for the Majorana sector. However, our numerical results are fairly similar. Two large mixing angles are found between 5% and 15% of the time as we change  $\Lambda_{Maj}$  and when we consider output masses similar to those needed experimentally. Note that the definition of “large mixing angles” is more generous in the anarchy papers ( $\sin^2 2\theta > 0.5$ ) than in our work ( $\sin^2 2\theta > 0.75$ ). In our simulations this can make a factor of two difference in the percentage of cases that are said to have two large mixing angles. For example, with  $\Lambda_{Maj} = 10^{12}$  GeV, the percentage of two large mixing angle solutions goes from 5.4% to 10.1% when adopting the more generous range. However, this does not change our conclusions. Large mixing angles are found a significant fraction of the time, but are not the most probable solution.

Our work has concentrated on the standard seesaw mechanism. If considering the Type II seesaw [23] or triplet seesaw [24] mechanisms instead, the neutrino mass matrix is completely determined by physics at a very high scale for which we have no basis to prefer a certain weight. This leads to more freedom because of the lack of constraints, but unfortunately also to no predictive power.

## 6 Summary and discussion

We have provided an exploration of the distribution of quark and lepton masses and mixings, treating these as random variables distributed with respect to some probability distribution

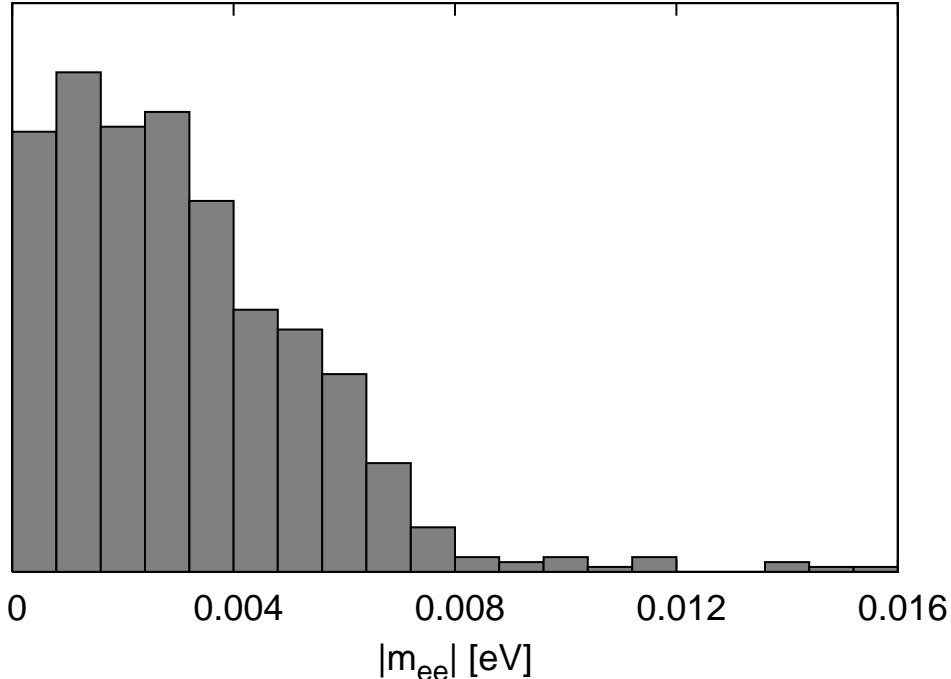


Figure 17: Distribution of the effective Majorana mass  $m_{ee}$

function, which we called the weight. We have shown that this weight is close to being scale invariant in form, i.e  $\rho(m) \sim 1/m$ . In particular a statistical analysis of power law weights  $\rho \sim 1/m^\delta$  tightly constrains the power to be  $\delta = 1.02 \pm 0.08$ . Such weights commonly produce small mixing angles and a hierarchy of CKM elements. Our exploration of the neutrino sector was somewhat inconclusive. The use of the usual seesaw mechanism, combined with the expected weight for the Dirac masses, could marginally accommodate the observed mass differences and mixing angles, but the existence of large mixing angles was not a common occurrence in this framework. However, the neutrino sector does allow us to make statistical predictions of this framework. A normal hierarchy of neutrino masses is highly favored by the scale invariant weights. We saw that the leptonic Jarlskog invariant is typically of order  $10^{-2}$  and with 95% confidence greater than  $1.6 \times 10^{-3}$ . The third presently unmeasured MNS mixing angle  $\sin \theta_{13}$  is typically of order 0.1 and with 95% confidence it is larger than 0.04. The effective Majorana mass  $m_{ee}$  is typically of order 0.001 eV.

We are aware of many caveats about this procedure, and there are probably others that we do not enumerate. Some of these issues are:

1) Differences between quarks and leptons: The information that we have about the masses exists at low energy. However, it is likely that the fundamental input consists of parameters defined at a high energy scale. We explored the effect of this using only the Standard Model to run the Yukawa couplings to the GUT scale, and this did not modify any of our conclusions. However, we clearly do not know the physics at intermediate scales. If the intermediate physics only produces logarithmic running, the residual effect is also probably not large.

2) Generation structure: The assumption of statistical independence of all masses may fail in some obvious ways. The most suspect aspect is that we do not assume any correlation

between members of the same generation. In some grand unified theories, this is incorrect, leading for example to a relation between the  $\tau$  and  $b$  quark masses [21]. Perhaps in the fundamental theory the random distribution occurs separately for the average value of a generation's masses and for the ratio of masses. This pattern is distinct from that which we have assumed.

3) Anthropic constraints: In a landscape picture there are inevitable anthropic constraints. Some parameter sets that occur in the landscape do not allow the existence of life, and hence we could not find ourselves in a portion of the multiverse where these parameters occurred. These constraints may distort the mass distribution. We have provided an estimate of this effect in the discussion of quark and lepton masses, and it appears not to change our qualitative conclusions. We have not considered a possible anthropic constraint on neutrino masses [25], which would disfavor masses above 1 eV. In general, it is hard to fully explore the effect of anthropic constraints without having the full fundamental theory.

4) Other flavor symmetries: Many of the attempts to understand quark and lepton masses have focussed on adding extra flavor symmetries to the Standard Model. Our basic assumption asserts that vacua with these extra symmetries do not constitute a large part of the string theory landscape of vacua.

From these comments, it is clear that our investigation is a rather preliminary attempt at phenomenology in the context of the landscape. In the end, the only fully compelling procedure is to identify the fundamental theory, such as string theory, that leads to the landscape and fully solve it. With this solution in hand one can investigate directly those vacua that lead to the Standard Model and calculate the statistical features of those solutions. Then one can directly address the constraints and symmetries that occur due to intermediate scale physics and can assess whether the fundamental theory is statistically compatible with the data. However, such a “top down” solution is clearly very difficult and we are far from being able to accomplish it. In the meantime we need to tentatively explore the phenomenology from the “bottom up” as best we are able.

It is hoped that eventually this weight can be calculated from a more fundamental theory such as string theory. An illustrative example was given in Ref. [3], using the Intersecting Brane Worlds (IBW) construction of the Standard Model [4]. There, the Yukawa couplings arise from the a non-perturbative effect spanning the area between the intersections of three pairs of branes ( $A_{ijk}$ ), with the Yukawa interactions being exponentially suppressed in that area,

$$\Gamma_{ijk} = \Gamma_0 e^{-\frac{A_{ijk}}{2\pi\alpha'}} \quad (43)$$

up to a phase. In this case a flat distribution in the area  $\rho(A) \sim \text{constant}$  yields the scale invariant weight in masses. The range in the allowed values of the area translates into a finite range in the masses. It is possible that this exponential behavior could be a more general feature of the landscape. Of course, this relation does not fully explain the nearly scale invariant distribution in the masses, but only transfers the problem to the string scale to understand whether the distribution in the area is nearly flat. It would be interesting to explore possible dynamics that could produce an ensemble of Standard Model string vacua and assess the resulting effect on the distribution of masses.

## Acknowledgement

We would like to thank Guy Blaylock for valuable discussions. This work has been supported in part by the U.S. National Science Foundation.

## Appendix: The weight for $\Delta m^2$ and the Majorana scale

When we consider the neutrino masses by themselves without mixing, the light neutrino masses  $m_i$  are of the form

$$m_i = \frac{m_{D,i}^2}{M_M} \quad (44)$$

where we take  $M_M$  as a common scale. Using the scale invariant weight

$$\rho(m_{D,i}) = \frac{1}{\log \frac{m_*}{m_{low}}} \frac{1}{m_{D,i}} \Theta(m_{D,i} - m_{low}) \Theta(m_* - m_{D,i}) \quad (45)$$

for the Dirac masses, we derive the weight for the neutrino mass differences  $\Delta m_{ij}^2 = m_j^2 - m_i^2$  and use the physical data for a likelihood fit of the Majorana scale  $M_M$ .

As a first step let us calculate the weight for the neutrino masses  $m_i$  with the scale invariant random Dirac masses  $m_{D,i}$ :

$$\begin{aligned} \rho(m_i) &= \int dm_{D,i} \rho(m_{D,i}) \delta\left(\frac{m_{D,i}^2}{M_M} - m_i\right) \\ &= \frac{1}{2 \log \frac{m_*}{m_{low}}} \frac{1}{m_i} \Theta\left(m_i - \frac{m_{low}^2}{M_M}\right) \Theta\left(\frac{m_*^2}{M_M} - m_i\right) \\ &= \frac{1}{\log \frac{M_U}{M_L}} \frac{1}{m_i} \Theta(m_i - M_L) \Theta(M_U - m_i) \end{aligned} \quad (46)$$

where we defined  $M_L = \frac{m_{low}^2}{M_M}$  and  $M_U = \frac{m_*^2}{M_M}$  for simplicity. We see that the neutrino masses are also distributed with respect to a scale invariant weight. The lower and upper bounds are of course changed as we would expect and the result in Eq. (46) is automatically normalized since we started from a normalized weight.

As a next step we calculate the weight for the neutrino masses squared,  $\rho(m_i^2)$ . The calculation is analogous to the one for  $\rho(m_i)$  in Eq. (46) and the result is

$$\rho(m_i^2) = \frac{1}{\log \frac{M_U^2}{M_L^2}} \frac{1}{m_i^2} \Theta(m_i^2 - M_L^2) \Theta(M_U^2 - m_i^2). \quad (47)$$

With that we will calculate the weight for  $\Delta m_{ij}^2 = m_j^2 - m_i^2$ :

$$\begin{aligned} \rho(\Delta m_{ij}^2) &= \int dm_i^2 \int dm_j^2 \rho(m_i^2) \rho(m_j^2) \delta(m_j^2 - m_i^2 - \Delta m_{ij}^2) \\ &= \frac{1}{\left(\log \frac{M_U^2}{M_L^2}\right)^2} \frac{1}{|\Delta m_{ij}^2|} \log \frac{\left(M_U^2 - |\Delta m_{ij}^2|\right) \left(M_L^2 + |\Delta m_{ij}^2|\right)}{M_U^2 M_L^2} \end{aligned} \quad (48)$$

As we would expect,  $\rho(\Delta m_{ij}^2) = \rho(-\Delta m_{ij}^2) = \rho(|\Delta m_{ij}^2|)$ , meaning that there is no preferred sign for  $\Delta m_{ij}^2$ . The weight for  $\Delta m_{ij}^2$  is basically proportional to one over  $\Delta m_{ij}^2$  up to some logarithmic corrections. For the complete weight  $\rho(\Delta m_{ij}^2)$ , we need to include

the range of possible values of  $\Delta m_{ij}^2$  with a Theta function:

$$\rho(\Delta m_{ij}^2) = \frac{1}{\left(\log \frac{M_U^2}{M_L^2}\right)^2} \frac{1}{|\Delta m_{ij}^2|} \log \frac{\left(M_U^2 - |\Delta m_{ij}^2|\right) \left(M_L^2 + |\Delta m_{ij}^2|\right)}{M_U^2 M_L^2} \Theta(M_U^2 - M_L^2 - |\Delta m_{ij}^2|) \quad (49)$$

Again, we find that our result is automatically normalized. Recall that we defined  $M_L = \frac{m_{low}^2}{M_M}$  and  $M_U = \frac{m_*^2}{M_M}$  so that  $\rho(\Delta m_{ij}^2)$  depends on the Majorana scale  $M_M$  as well as on  $m_{low}$  and  $m_*$ . Our analytic result for  $\rho(\Delta m_{ij}^2)$  agrees exactly with the result of corresponding simulations.

One benefit of explicitly knowing the weight of an observable is that one can perform a likelihood fit with it. If we used the weight for  $\Delta m^2$  along with the physical data for  $\Delta m_{12}^2$  and  $\Delta m_{13}^2$  to fit the Majorana scale  $M_M$  using a likelihood function  $L = \rho(\Delta m_{12}^2) \rho(\Delta m_{13}^2)$ , we would make a mistake by assuming the two measured mass differences are independent of each other. Therefore we have to first calculate the weight for two neutrino mass differences  $\rho(\Delta m_{ij}^2, \Delta m_{ik}^2)$  that takes the correlation into account:

$$\begin{aligned} \rho(\Delta m_{ij}^2, \Delta m_{ik}^2) &= \int dm_i^2 \int dm_j^2 \int dm_k^2 \rho(m_i^2) \rho(m_j^2) \rho(m_k^2) \\ &\quad \delta(m_j^2 - m_i^2 - \Delta m_{ij}^2) \delta(m_k^2 - m_i^2 - \Delta m_{ik}^2) \\ &= \frac{1}{\left(\log \frac{M_U^2}{M_L^2}\right)^3} \int dm_i^2 \frac{1}{m_i^2} \frac{1}{m_i^2 + \Delta m_{ij}^2} \frac{1}{m_i^2 + \Delta m_{ik}^2} \\ &\quad \Theta(m_i^2 - M_L^2) \Theta(M_U^2 - m_i^2) \\ &\quad \Theta(m_i^2 - (M_L^2 - \Delta m_{ij}^2)) \Theta((M_U^2 - \Delta m_{ij}^2) - m_i^2) \\ &\quad \Theta(m_i^2 - (M_L^2 - \Delta m_{ik}^2)) \Theta((M_U^2 - \Delta m_{ik}^2) - m_i^2) \\ &= \frac{1}{\left(\log \frac{M_U^2}{M_L^2}\right)^3} \left[ \frac{1}{\Delta m_{ij}^2 \Delta m_{ik}^2} \log \frac{M_U^2 - \Delta m_{ik}^2}{M_L^2} \right. \\ &\quad + \frac{1}{\Delta m_{ij}^2 (\Delta m_{ij}^2 - \Delta m_{ik}^2)} \log \frac{M_U^2 - \Delta m_{ik}^2 + \Delta m_{ij}^2}{M_L^2 + \Delta m_{ij}^2} \\ &\quad \left. + \frac{1}{\Delta m_{ik}^2 (\Delta m_{ik}^2 - \Delta m_{ij}^2)} \log \frac{M_U^2}{M_L^2 + \Delta m_{ik}^2} \right] \\ &\quad \Theta(\Delta m_{ik}^2) \Theta((M_U^2 - M_L^2) - \Delta m_{ik}^2) \\ &\quad \Theta(\Delta m_{ik}^2) \Theta(\Delta m_{ik}^2 - \Delta m_{ij}^2) + \dots \end{aligned} \quad (50)$$

Here we only display the part of the result for the case where  $0 < \Delta m_{ij}^2 < \Delta m_{ik}^2$  which is the case for a normal neutrino mass hierarchy when we identify  $\Delta m_{ij}^2$  with  $\Delta m_{12}^2$  and  $\Delta m_{ik}^2$  with  $\Delta m_{13}^2$ . Again, this weight depends on the Majorana scale  $M_M$  via  $M_L$  and  $M_U$ .

Now we can finally perform a likelihood fit for the Majorana scale  $M_M$  using the likelihood function  $L(M_M) = \rho(\Delta m_{12}^2, \Delta m_{13}^2)$ . As the experimental input we use the central values [22]  $\Delta m_{12}^2 = 8.0 \times 10^{-5} \text{ eV}^2$  and  $\Delta m_{13}^2 = 2.3 \times 10^{-3} \text{ eV}^2$ . We find that  $M_M$  has to be smaller than  $10^{15} \text{ GeV}$  to accommodate the experimental data. As a preferred value the

fit yields  $9 \times 10^{14}$  GeV. At the  $1\sigma$  level  $M_M < 3 \times 10^{10}$  GeV are excluded and at the  $2\sigma$  level  $M_M < 10^5$  GeV are excluded.

To interpret these results it is useful to have a second look at Fig. 14 where we assume hierarchical neutrino masses  $m_1 \ll m_2 \ll m_3$ . For high  $M_M$  there is more “phase space” for the lightest neutrino mass which explains the preferred value close to its upper limit. But since this “phase space” decreases only linearly when one goes to smaller  $M_M$  on a logarithmic scale the the range of allowed Majorana scales  $M_M$  spans many orders of magnitude.

## References

- [1] J. F. Donoghue, “The weight for random quark masses,” Phys. Rev. D **57**, 5499 (1998) [arXiv:hep-ph/9712333].
- [2] M. R. Douglas, “The statistics of string / M theory vacua,” JHEP **0305**, 046 (2003) [arXiv:hep-th/0303194].  
 S. Ashok and M. R. Douglas, “Counting flux vacua,” arXiv:hep-th/0307049.  
 L. Susskind, “The anthropic landscape of string theory,” arXiv:hep-th/0302219.  
 T. Banks, M. Dine and E. Gorbatov, “Is there a string theory landscape?,” arXiv:hep-th/0309170  
 R. Kallosh and A. Linde, “M-theory, cosmological constant and anthropic principle,” Phys. Rev. D **67**, 023510 (2003) [arXiv:hep-th/0208157].  
 R. Bousso and J. Polchinski, “Quantization of four-form fluxes and dynamical neutralization of the cosmological constant,” JHEP **0006**, 006 (2000) [arXiv:hep-th/0004134].
- [3] J. F. Donoghue, “Dynamics of M theory vacua”, Phys. Rev. D **69**, 106012 (2004) [Erratum-ibid. D **69**, 129901 (2004)] [arXiv:hep-th/0310203].
- [4] D. Cremades, L. E. Ibanez and F. Marchesano, “Towards a theory of quark masses, mixings and CP-violation,” arXiv:hep-ph/0212064.  
 D. Cremades, L. E. Ibanez and F. Marchesano, “Yukawa couplings in intersecting D-brane models,” JHEP **0307**, 038 (2003) [arXiv:hep-th/0302105].
- [5] B. Pendleton and G. G. Ross, “Mass And Mixing Angle Predictions From Infrared Fixed Points,” Phys. Lett. B **98**, 291 (1981).  
 C. T. Hill, “Quark And Lepton Masses From Renormalization Group Fixed Points,” Phys. Rev. D **24**, 691 (1981).  
 C. T. Hill, C. N. Leung and S. Rao, “Renormalization Group Fixed Points And The Higgs Boson Spectrum,” Nucl. Phys. B **262**, 517 (1985).  
 M. Lanzagorta and G. G. Ross, “Infrared fixed points revisited,” Phys. Lett. B **349**, 319 (1995) [arXiv:hep-ph/9501394].
- [6] J. Barrow and F. Tipler, *The Anthropic Cosmological Principle* (Clarendon Press, Oxford, 1986).  
 C.J. Hogan, “Why the universe is just so,” astro-ph/9909295.  
 R. N. Cahn, “The eighteen arbitrary parameters of the standard model in your everyday life,” Rev. Mod. Phys. **68**, 951 (1996).  
 L. B. Okun, Usp. Phys. Nauk, **161**, 177 (1991)(Soviet Phys. Usp. **34**, 818)

- [7] V. Agrawal, S.M. Barr, J.F. Donoghue and D. Seckel, “Anthropic considerations in multiple-domain theories and the scale of electroweak symmetry breaking,” *Phys. Rev. Lett.* **80**, 1822 (1998) hep-ph/9801253.  
V. Agrawal, S.M. Barr, J.F. Donoghue and D. Seckel, “The anthropic principle and the mass scale of the standard model,” *Phys. Rev.* **D57**, 5480 (1998) hep-ph/9707380.
- [8] T. Damour and J.F. Donoghue (to appear)
- [9] J.F. Donoghue, E. Golowich and B.R. Holstein, *Dynamics of the Standard Model* (Cambridge University Press, 1992)
- [10] S. Eidelman *et al.* [Particle Data Group], “Review of particle physics,” *Phys. Lett. B* **592**, 1 (2004).
- [11] H. Fritzsch and Z. z. Xing, “Mass and flavor mixing schemes of quarks and leptons,” *Prog. Part. Nucl. Phys.* **45**, 1 (2000) [arXiv:hep-ph/9912358].
- [12] C. Jarlskog, “Commutator Of The Quark Mass Matrices In The Standard Electroweak Model And A Measure Of Maximal CP Violation,” *Phys. Rev. Lett.* **55**, 1039 (1985).
- [13] M. Gell-Mann, P. Ramond and R. Slansky, “Color Embeddings, Charge Assignments, And Proton Stability In Unified Gauge Theories,” *Rev. Mod. Phys.* **50**, 721 (1978).
- [14] R. N. Mohapatra *et. al.*, “Theory of Neutinos”, hep-ph/0412099.
- [15] D. N. Spergel *et al.* [WMAP Collaboration], “First Year Wilkinson Microwave Anisotropy Probe (WMAP) Observations: Determination of Cosmological Parameters,” *Astrophys. J. Suppl.* **148**, 175 (2003) [arXiv:astro-ph/0302209].
- [16] A. Datta, F. S. Ling and P. Ramond, “Correlated hierarchy, Dirac masses and large mixing angles,” *Nucl. Phys. B* **671**, 383 (2003) [arXiv:hep-ph/0306002].
- [17] J. N. Bahcall, M. C. Gonzalez-Garcia and C. Pena-Garay, “Solar neutrinos before and after Neutrino 2004,” *JHEP* **0408**, 016 (2004) [arXiv:hep-ph/0406294].
- [18] T. Goldman and G. J. Stephenson, “How Large Are The Neutrino Mixing Angles?,” *Phys. Rev. D* **24**, 236 (1981).
- [19] L. J. Hall, H. Murayama and N. Weiner, “Neutrino mass anarchy,” *Phys. Rev. Lett.* **84**, 2572 (2000) [arXiv:hep-ph/9911341].  
N. Haba and H. Murayama, “Anarchy and hierarchy,” *Phys. Rev. D* **63**, 053010 (2001) [arXiv:hep-ph/0009174].  
A. de Gouvea and H. Murayama, “Statistical test of anarchy,” *Phys. Lett. B* **573**, 94 (2003) [arXiv:hep-ph/0301050].  
J. R. Espinosa, “Anarchy in the neutrino sector?,” arXiv:hep-ph/0306019.
- [20] S. M. Bilenky, “Neutrinoless double beta-decay: Status and future,” arXiv:hep-ph/0509098.
- [21] H. Georgi and C. Jarlskog, “A New Lepton - Quark Mass Relation In A Unified Theory,” *Phys. Lett. B* **86**, 297 (1979).

- [22] S. Goswami, “Neutrino oscillations and masses,” Talk at Lepton-Photon 2005, [<http://lp2005.tsl.uu.se/~lp2005/>].  
M. Maltoni, T. Schwetz, M. A. Tortola and J. W. F. Valle, “Status of global fits to neutrino oscillations,” *New J. Phys.* **6**, 122 (2004) [arXiv:hep-ph/0405172].
- [23] R. N. Mohapatra and G. Senjanovic, “Neutrino Masses And Mixings In Gauge Models With Spontaneous Parity Violation,” *Phys. Rev. D* **23**, 165 (1981).  
G. Lazarides, Q. Shafi and C. Wetterich, “Proton Lifetime And Fermion Masses In An SO(10) Model,” *Nucl. Phys. B* **181**, 287 (1981).  
J. Schechter and J. W. F. Valle, “Neutrino Masses In SU(2) X U(1) Theories,” *Phys. Rev. D* **22**, 2227 (1980).  
J. Schechter and J. W. F. Valle, “Neutrino Decay And Spontaneous Violation Of Lepton Number,” *Phys. Rev. D* **25**, 774 (1982).
- [24] T. P. Cheng and L. F. Li, “Neutrino Masses, Mixings And Oscillations In SU(2) X U(1) Models Of Electroweak Interactions,” *Phys. Rev. D* **22**, 2860 (1980).
- [25] M. Tegmark, A. Vilenkin and L. Pogosian, “Anthropic predictions for neutrino masses,” *Phys. Rev. D* **71**, 103523 (2005) [arXiv:astro-ph/0304536].